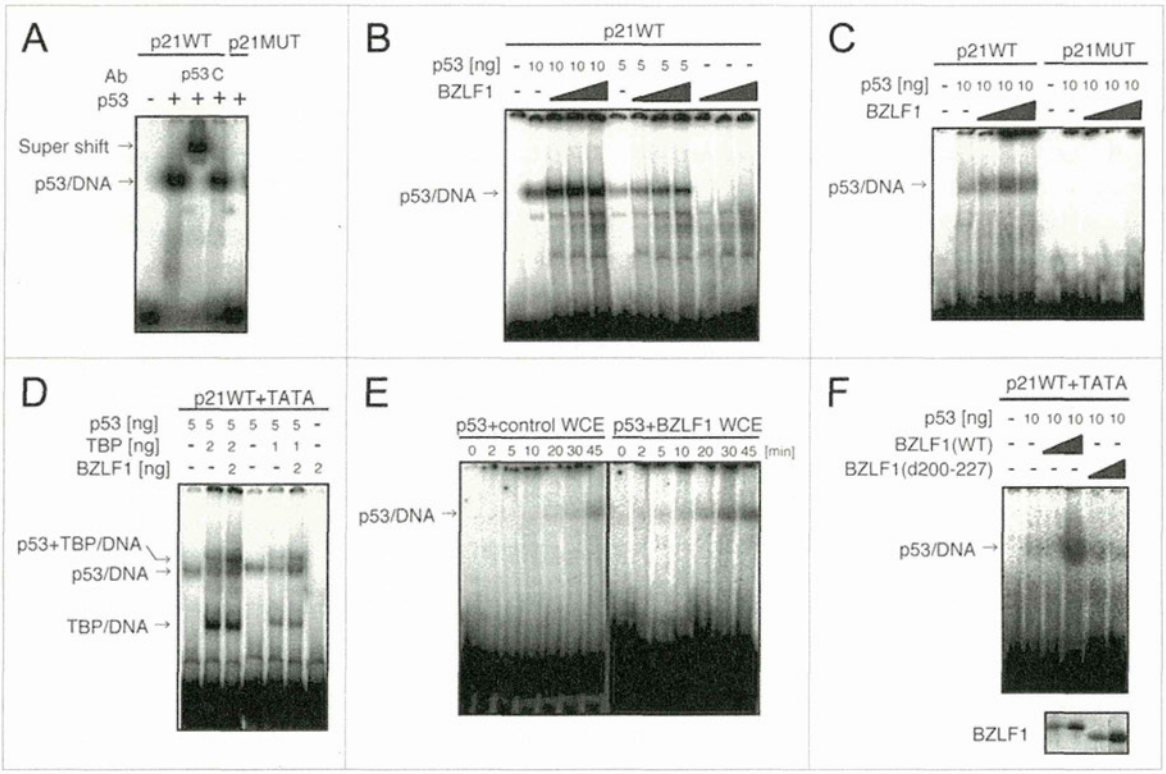


**Figure 3.** The BZLF1 protein enhances binding of p53 to DNA at an association step. (A) p53 binds to its consensus sequence in the *p21*$^{WAF1/CIP1}$ promoter. Super shift assays were performed with the p21WT probe containing a p53-binding site and the p21MUT probe containing a mutation in the p53 consensus sequence as described in the Experimental Procedures. Ten ng of HA-p53 recombinant protein, and 1 μg of control mouse IgG (C) or p53 monoclonal (p53) antibodies were used. (B) DNA-binding activity of p53 is stimulated by BZLF1 protein. EMSA was performed with HA-p53 protein (10 or 5 ng), increasing amounts of whole cell extract (BZLF1 WCE) from Sf21 cells infected with AcBZLF1 and $^{32}$P-labeled p21WT as a probe. The bands below the p53/DNA complex are non-specific. (C) BZLF1 protein enhances p53 DNA-binding in a consensus sequence-specific manner. EMSA was performed with HA-p53 protein (10 ng), increasing amounts of whole cell extract (BZLF1 WCE) from Sf21 cells infected with AcBZLF1 and $^{32}$P-labeled p21WT or p21MUT probes. (D) Stimulation of the recruitment of TBP to p53/DNA complex by BZLF1 protein. EMSA was performed with recombinant HA-p53 (5 ng), TBP (1 or 2 ng) and BZLF1 protein (2 ng), with $^{32}$P-labeled p21WT-TATA as a probe. Arrows indicate p53 + TBP/DNA, p53/DNA and TBP/DNA complexes formed (top to bottom). (E) BZLF1 protein enhances the association of p53 with its binding site in the promoter. EMSA was performed with $^{32}$P-labeled p21WT as a probe for determination of association rates of p53/DNA complexes. DNA-binding reactions were performed in the presence of WCE containing BZLF1 protein for different times. As a control, the same amount of WCE from Sf21 cells infected with AcMCM7 was used. (F) Interaction between p53 and the BZLF1 protein is required for the enhancement of p53-DNA binding. EMSA was performed with $^{32}$P-labeled p21WT-TATA as a probe using purified recombinant HA-p53 (10 ng) and either wild-type BZLF1 protein or d200-227 lacking the association with p53. Purified BZLF1 proteins were subjected to SDS-PAGE followed by Coomassie blue staining.

not affect the dissociation rates of p53-DNA complex when the p53-DNA complexes were challenged with 20-fold molar excess of unlabeled p21WT probe as a competitor (data not shown).

To further test whether the association of BZLF1 protein to p53 is required for the enhancement of the p53 DNA-binding activity, we performed EMSA using a BZLF1 mutant, d200-227 mutant which cannot bind to p53.[25] As shown in **Figure 3F**, the BZLF1 d200-227 mutant did not enhance the p53 DNA-binding activity at all. This finding indicates that the physical interaction between p53 and BZLF1 protein is required for the BZLF1-mediated enhancement of p53 DNA-binding activity. These results suggest that BZLF1 interacts with p53, thereby enhancing the p53 binding to its recognition element.

**BZLF1 protein enhances p53-mediated transcription in vitro.** According to these observations, it is most likely that BZLF1 protein stimulates p53-dependent transcription in vitro. Therefore, we carried out in vitro transcription assay using HeLa nuclear extracts. The linearized PG13-Luc reporter plasmid, containing 13 copies of p53 DNA binding sites upstream of a basal promoter linked to a luciferase reporter gene,[3] was used as a template DNA, and the linearized DNA of pcDNA4 was used as an internal control (**Fig. 4**). The amounts of the transcripts were measured by primer extension analysis with $^{32}$P-labeled primer. The expected sizes of the primer extension products are 130 and 60 nucleotide lengths, respectively. As shown in **Figure 4**, the addition of p53 protein specifically activated transcription from the template with p53 binding sites (PG13-Luc; *lane 3*), and the addition of BZLF1 protein further enhanced the transcription (PG13-Luc; *lane 4 and 5*). In contrast, the levels of pcDNA4-transcription were unaffected (pcDNA4; *lane 6–9*). These data clearly demonstrate that the BZLF1 protein stimulates p53-dependent transcription in vitro.

**Transactivation of p53-target genes correlates with occupancy of p53 at its promoter.** To validate the effect of BZLF1

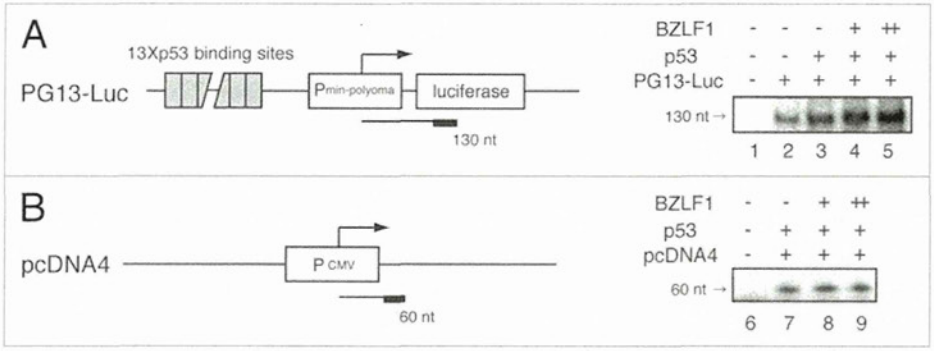


**Figure 4.** Cooperation between p53 and the BZLF1 protein activates p53-specific transcription in vitro. In vitro transcription templates used are indicated (*left*). PG13-Luc contains thirteen copies of p53 binding sites upstream of the polyoma virus minimum promoter and the luciferase gene. This template is responsive to activation of p53. pcDNA4 containing CMV IE promoter was used as a control for the reactions. These templates were linearized by the restriction enzyme digestion. In vitro transcription reaction mixtures contained HeLa nuclear extract, linearized template DNA, p53 protein (15 ng) and purified BZLF1 protein (4 or 10 ng). In vitro transcription and primer extension were performed as described in the Experimental Procedures, the primer extension products of RNAs transcribed from PG13-Luc (A) and pcDNA4 (B) are 130 nucleotides (130 nt) and 60 nucleotides (60 nt) in length, respectively.

protein on the p53 DNA-binding activity in vivo, we utilized Tet-BZLF1/HeLa cells and examined the effect of BZLF1 expression on the dynamics of p53 binding to its target promoters (*p21*$^{WAF1/CIP1}$ and *p53* promoter)[26] by ChIP assay. As shown in **Figure 5**, following the induction of the BZLF1 protein, p53 protein was found to bind to both the *p21*$^{WAF1/CIP1}$ and p53 promoter regions. This observation corresponds well with the expression pattern of *p21*$^{WAF1/CIP1}$- and *p53*-gene transcripts following the induction of BZLF1 protein (**Fig. 2B**). These findings imply that BZLF1 protein induces the transactivation of p53 by stimulating the p53 protein binding to its recognition sequences in vivo. Induction of p53 should form a positive feedback loop regaling the p53 expression and should lead to amplification of p53-downstream signaling.[26-28]

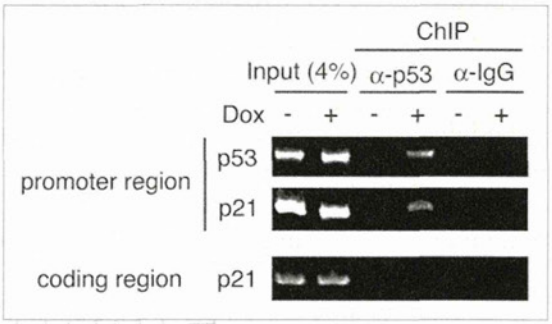


**Figure 5.** BZLF1 protein induces the recruitment of p53 to its target promoters. ChIP assays were performed with Tet-BZLF1/HeLa cells. The *p53* and *p21*$^{WAF1/CIP1}$ promoter and *p21*$^{WAF1/CIP1}$ coding region were detected by PCR amplification. IgG was used for a negative control.

## Discussion

Previous studies demonstrated that the EBV immediate-early protein BZLF1, which was either conditionally-expressed[15,16] or was overexpressed by a recombinant adenovirus[21,29] could induce $G_1$ arrest in some cell lines. The BZLF1 protein caused the accumulation of both mRNA and protein of CDK inhibitor p21$^{WAF1/CIP1}$,[15] a well-known p53-target gene product. Thus, it appears that the BZLF1 protein affects p21 expression through transcriptional regulation.

In this study, we investigated the mechanism by which the BZLF1 protein enhances p53-dependent transactivation. Our data demonstrate the BZLF1 enhances the p53-DNA binding by accelerating the p53-DNA complex formation. Enhanced p53 binding to its genomic recognition sequences enables the efficient expression of p53-target genes, including p21$^{WAF1/CIP1}$ and p53 itself, which, in turn, causes cell cycle arrest in epithelial cells. Our study has clarified the pathway that links between the BZLF1 expression and the induction of p53-target genes.

However, we cannot rule out another possibility that the BZLF1 protein cooperates with bZIP transcription factor C/EBPα to promote cell cycle arrest. A group of Hayward found that BZLF1 protein protects C/EBPα from proteasome-dependent degradation.[30] Since C/EBPα auto-regulates its own promoter, this rapidly results in enhanced C/EBPα expression. In addition, C/EBPα transactivates p21$^{WAF1/CIP1}$. Thus, BZLF1 protein causes $G_1$ arrest through the interaction with C/EBPα. Moreover, the activation domain of BZLF1 protein also contributes to transactivates p27$^{KIP1}$.[31] These results including this study suggest involvement of more than one mechanism behind the BZLF1 protein-mediated cell cycle arrest.

During the course of lytic replication, we propose that BZLF1 protein plays two distinctive roles in the regulation of p53-mediated transactivation depending on the phosphorylation states of p53. In the early phases of lytic replication, p53 is mainly in the hypo-phosphorylated form.[9] In general, the hypo-phosphorylated form of p53 exhibits weak DNA binding to its recognition sequences and is transcriptionally-inactive. The BZLF1 protein helps the hypo-phosphorylated p53 to bind to its recognition sequences, leading to the enhancement of p53 dependent transcription. This results in the transient increase in levels of p21$^{WAF1/CIP1}$, which causes the cell cycle arrest at the early stages of the lytic replication. By contrast, at middle and late stages of lytic replication, the phosphorylation state of p53 dramatically

changes. When viral genome DNAs are synthesized after 24 h.p.i., the host cell DNA damage-sensing machinery recognizes the viral DNA as an abnormal DNA structures, activating ATM dependent DNA damage signaling. ATM, in turn, phosphorylates p53 at various sites including S15,[9] which liberates p53 from MDM2-mediated degradation. Instead, another pathway to degrade p53 protein becomes active. We have recently found that induction of EBV lytic program leads to the degradation of p53 via an ubiquitin-proteasome pathway, which is independent of MDM2.[19] The BZLF1 protein directly functions as an adaptor component of the ECS ubiquitin ligase complex targeting phosphorylated p53 for degradation.[10] As a result, the p53 target gene products are maintained at very low levels, and host cells are maintained in S-phase like condition,[9,19,32] which appears to be important for the progression of lytic replication. Supporting the idea, compensating the expression of p53 at middle to late stages of the lytic infection inhibits viral DNA replication and virus production during lytic infection.[10] This is in contrast to our observation that p53 expression enhanced viral genome replication at the early stages of infection. Overall, BZLF1 enables hypo-phosphorylated p53 to transactivate its target genes in the initial phase of lytic replication, while the acitivated p53 is degraded to maintain S-phase like environment for the efficient propagation of lytic replication at the later stages.

It is raised why p53 is required for viral proliferation at the early stages of the lytic infection. Several studies regarding p53 and human cytomegalovirus (HCMV), a member of beta-herpesvirus family, have demonstrated the elevated levels of p53 protein upon viral infection, whereas the cellular downstream targets of p53 are not activated.[33,34] It was reported that cells infected with HCMV in the absence of p53 produced fewer infectious viral particles, and that the loss of p53 caused the delays of viral protein production and its trafficking.[33] The observed delayed formation of replication centers could result in the delay of viral encapsidation.[33] Interestingly, HCMV genome has 21 potential p53 responsible sites.[35] HCMV genome-bound p53 molecules were most influential on HCMV gene expression at immediate-early and early stages of postinfection, implying a mechanism for the reduced and delayed production of virions in $p53^{-/-}$ cells. Similarly, potential p53 recognition sequences were also present on EBV genome (Murata T, et al. unpublished results). We showed previously that p53 is associated with EBV replication compartments.[9] Thus, it is tempting to speculate that p53 is recruited to EBV replication compartment through its direct binding to the recognition sequences within the EBV genome. Overall, the BZLF1-meditaed enhancement of p53-DNA binding may contribute to the stimulated expression of viral genes that are transactivated by p53 at early stages of EBV lytic infection.

## Experimental Procedures

**Cloning of Tet-BZLF1/Hela cells.** To generate Tet-BZLF1/HeLa cells, HeLa Tet-on cells (Clontech) was transfected with pCMSCV-RevTRE(hyg)-BZLF1.[32] Stable clones were obtained by double selection in the presence of G418 and hygromycin B. Clones resistant to G418 and hygromycin B were isolated by limiting dilution and checked for expression of the BZLF1 with doxycline by immunoblotting analysis.

**Cells and regents.** Tet-BZLF1/HeLa cells were cultured in D-MEM containing 10% tetracycline free fetal calf serum in the presence of G418 and hygromycin B. Tet-BZLF1/B95-8 cells were maintained in RPMI medium containing 10% tetracycline free fetal calf serum in the presence of puromycin and hygromycin B.[32] To induce BZLF1 protein expression, the tetracycline derivative doxycycline (Dox) was added to the culture medium at a final concentration of 1 μg/ml. The anti-p53 (FL-393) and anti-$p21^{WAF1/CIP1}$ (C19G) antibodies were purchased from Santa Cruz Biotechnology. Affinity-purified anti-BZLF1 protein antibody was prepared as described previously.[36]

**Preparation of whole cell extracts.** Whole cell extracts (WCE) of Sf21 cells infected with the recombinant baculovirus expressing BZLF1 protein, AcBZLF1, were prepared as follows. Sf21 cells were infected with AcBZLF1 at a M.O.I. of 10, harvested 72 h postinfection, and suspended in insect cell lysis buffer (50 mM Tris-HCl pH 7.6, 150 mM NaCl, 1% NP40, 1 mM DTT) containing a protease inhibitor cocktail. After 60 min incubation on ice, cell lysates were centrifuged and the supernatant was collected. As a control, whole cell extracts were also prepared similarly from Sf21 cells infected with the recombinant baculovirus expressing human MCM7, AcMCM7.

**Purification of proteins.** Purified TBP protein was purchased from Wako. HA-tagged p53 was expressed in Sf21 cells infected with recombinant baculovirus[22] that were kindly provided by Dr. C. Prives (Columbia University). HA-p53 protein was purified using monoclonal anti-HA agarose conjugate (Sigma) and elution was performed using HA peptide (Sigma). Purification of EBV BZLF1 protein was described previously.[10]

**Electrophoretic mobility shift assay (EMSA).** Gel mobility shift assays were carried out as described previously,[22] with some modifications. The p21WT and p21MUT probes were oligonucleotides containing the wild-type p53 consensus site in the $p21^{WAF1/CIP1}$ gene promoter[37] and mutant sequences,[38] respectively. The p21WT-TATA probe was a 130-bp DNA fragment generated by digestion with KpnI and XbaI of pBluescript II KS (Stratagene) including the p21WT probe sequence at the EcoRI site and the TATA box sequence (5'-CCT GTT ATA AAA GCA GTG-3') between PstI and BamHI sites. The probes were $^{32}$P-labeled by the Klenow fragment of *E. coli* DNA polymerase I. Reaction mixtures (20 μl) contained 20 mM HEPES, pH 7.9, 25 mM KCl, 0.1 mM EDTA, 2 mM $MgCl_2$, 0.5 mM DTT, 10% (v/v) glycerol, 2 mM spermidine, 0.025% NP40, 0.5 μg of double-stranded poly(dG-dC), 2 μg of BSA, 0.15 pmol of $^{32}$P-labeled probe DNA, and protein samples and reactions were carried out at room temperature for 40 min. The amount of WCE was kept constant by adding control MCM7 WCE. For antibody supershift assays, 1 μg of antibody was added directly to the reaction mixtures, followed by incubation for 15 min. DNA-protein complexes were analyzed on native 4% polyacrylamide gels containing 0.5x Tris-borate-EDTA (TBE) buffer and 0.05% NP40 and were quantified by BAS 2500 Imaging analyzer (Fuji Photo Film). When experiments for association rate of p53-DNA were performed, incubation was for the indicated

times and then immediately applied for gel electorophoresis. For dissociation experiments, incubation was for 30 min, immediately followed by addition of a 20-fold excess of unlabeled p21WT oligonucleotide to challenge the DNA-protein complex for the indicated times. The mixture was then applied for gel electorophoresis.

**In vitro transcription and primer extension.** In vitro transcription assays with nuclear extract were performed using the HeLaScribe nuclear extract in vitro transcription system (Promega) following the manufacturer's protocol. Briefly, reactions (25 µl) contained 20 mM HEPES (pH 7.9), 5 mM $MgSO_4$, 0.2 mM EGTA, 20% glycerol, 0.5 mM DTT, 100 mM KCl, with nucleotide ribo-triphosphates (0.4 mM each), 8 U of HeLa nuclear extract, recombinant proteins and 0.3 µg of PG13-Luc reporter plasmid, or 0.1 µg of pcDNA4A plasmid (Invitrogen). PG13-Luc[3] was gifts from Dr. B. Vogelstein (The Johns Hopkins University Medical Institutions). The reactions were allowed to proceed for 15 min at 30°C. Primer extension analysis for the RNA produced during these reactions was performed using a $\gamma$-$^{32}$P 5'-end-labeled oligonucleotide complementary to the luciferase coding sequence (5'-GAA GAG CCA AAA AC-3') and the pcDNA4 vector sequence (5'-TCG TTT AGT GAA CCG TCA GAT-3') as a control. The extension products were separated on a 8% polyacrylamide gel containing 0.5x TBE and 7 M urea, analyzed by autoradiography, and quantified with a BAS 2500 Imaging analyzer (Fuji Photo Film).

**Luciferase reporter assay.** Tet-BZLF1/HeLa cells seeded in 24-well plates were transfected with 0.05 µg of the luciferase reporter plasmid (PG13-Luc), and treated with or without Dox. The amount of transfected DNA was kept constant by adding empty vector. Luciferase activity was measured with a luciferase assay system (Promega) according to the manufacturer's instructions, using a luminometer (Berthold).

**RT-PCR analysis.** Isolation of total RNA from cells was performed using RNeasy spin column kits (Qiagen) and cDNAs were synthesized using SuperScript III first-strand synthesis system for RT-PCR (Invitrogen) with total RNAs as templates. The detection of *GAPDH*, *p53* and *p21$^{WAF1/CIP1}$* cDNAs was performed by PCR using as primers; 5'-GGG AAG GTG AAG GTC GGA GT-3' and 5'-AAG ACG CCA GTG GAC TCC AC-3' for GAPDH, 5'-CCC AAC AAC ACC AGC-3' and 5'-GTG GCT GGA GTG AGC-3' for p53, and 5'-GCC CAG TGG ACA GCG AGC AG-3' and 5'-ATC TGT CAT GCT GGT CTG CC-3' for *p21$^{WAF1/CIP1}$*. *GAPDH*, *p53* and *p21$^{WAF1/CIP1}$* were amplified for 17, 30 and 26 cycles, respectively. The GAPDH gene served as an internal control in the calculation of the densitometric results.

**ChIP assay.** Immunoprecipitation of formaldehyde-cross-linked chromatin from the Dox-induced Tet-BZLF1/HeLa cells was performed as described previously.[39] The immunoprecipitated DNAs and input DNA were analyzed by PCR using the following as primers; 5'-TTC CTC TGA AAG CTG ACT GCC-3' and 5'-CAT GTT CCT GAC GGC CAG A-3' for the *p21$^{WAF1/CIP1}$* promoter region, 5'-CAG AGT GAT AAG GGT TGT GAA GGA G-3' and 5'-AAA ACC CCA ATC CCA TCA ACC-3' for the *p53* promoter region, and 5'-CAG GAG GCC CGT GAG CGA TGG A-3' and 5'-CTG TCC CCT GCA GCA GAG CAG GTG-3' for the *p21$^{WAF1/CIP1}$*-coding region.

**Quantification of viral DNA synthesis during lytic replication.** Tet-BZLF1/B95-8 cells were transfected with p53 expression plasmid or GFP-expression plasmid as a control by electroporation and then added doxycycline into the culture media 1 h post-transfection for induction of the lytic replication. Dot-blot hybridization and viral genome replication was quantified as described previously.[10]


### Acknowledgements

We are grateful to Drs. C. Prives, B. Vogelstein and K. Kuzushima for invaluable materials. We thank Yasuhiro Nishikawa and Kiyoko Sasaki for technical assistance. This study was supported in part by Grants-in-aid for Scientific Research on Priority Areas from the Ministry of Education, Science, Sports, Culture and Technology of Japan (no. 21022055, 20012056, 20390137 to T.T.). Y.S. was supported by the Japanese Society for a Research Fellowship of the Promotion of Science for Young Scientists.


### References


1. Haffner R, Oren M. Biochemical properties and biological effects of p53. Curr Opin Genet Dev 1995; 5:84-90.
2. Ko LJ, Prives C. p53: puzzle and paradigm. Genes Dev 1996; 10:1054-72.
3. el-Deiry WS, Tokino T, Velculescu VE, Levy DB, Parsons R, Trent JM, et al. WAF1, a potential mediator of p53 tumor suppression. Cell 1993; 75:817-25.
4. Dulic V, Kaufmann WK, Wilson SJ, Tlsty TD, Lees E, Harper JW, et al. p53-dependent inhibition of cyclin-dependent kinase activities in human fibroblasts during radiation-induced $G_1$ arrest. Cell 1994; 76:1013-23.
5. Tsurumi T. EBV replication enzymes. Curr Top Microbiol Immunol 2001; 258:65-87.
6. Chien YC, Chen JY, Liu MY, Yang HI, Hsu MM, Chen CJ, et al. Serologic markers of Epstein-Barr virus infection and nasopharyngeal carcinoma in Taiwanese men. N Engl J Med 2001; 345:1877-82.
7. Zeng Y, Zhang LG, Wu YC, Huang YS, Huang NQ, Li JY, et al. Prospective studies on nasopharyngeal carcinoma in Epstein-Barr virus IgA/VCA antibody-positive persons in Wuzhou City, China. Int J Cancer 1985; 36:545-7.
8. Hong GK, Gulley ML, Feng WH, Delecluse HJ, Holley-Guthrie E, Kenney SC. Epstein-Barr virus lytic infection contributes to lymphoproliferative disease in a SCID mouse model. J Virol 2005; 79:13993-4003.
9. Kudoh A, Fujita M, Zhang L, Shirata N, Daikoku T, Sugaya Y, et al. Epstein-Barr virus lytic replication elicits ATM checkpoint signal transduction while providing an S-phase-like cellular environment. J Biol Chem 2005; 280:8156-63.
10. Sato Y, Kamura T, Shirata N, Murata T, Kudoh A, Iwahori S, et al. Degradation of Phosphorylated p53 by Viral Protein-ECS E3 Ligase Complex. PLoS Pathog 2009; 5:1000530.
11. Rooney CM, Rowe DT, Ragot T, Farrell PJ. The spliced BZLF1 gene of Epstein-Barr virus (EBV) transactivates an early EBV promoter and induces the virus productive cycle. J Virol 1989; 63:3109-16.
12. Urier G, Buisson M, Chambard P, Sergeant A. The Epstein-Barr virus early protein EB1 activates transcription from different responsive elements including AP-1 binding sites. EMBO J 1989; 8:1447-53.
13. Farrell PJ, Rowe DT, Rooney CM, Kouzarides T. Epstein-Barr virus BZLF1 trans-activator specifically binds to a consensus AP-1 site and is related to c-fos. EMBO J 1989; 8:127-32.
14. Takagi S, Takada K, Sairenji T. Formation of intranuclear replication compartments of Epstein-Barr virus with redistribution of BZLF1 and BMRF1 gene products. Virology 1991; 185:309-15.
15. Cayrol C, Flemington EK. The Epstein-Barr virus bZIP transcription factor Zta causes $G_0/G_1$ cell cycle arrest through induction of cyclin-dependent kinase inhibitors. EMBO J 1996; 15:2748-59.
16. Cayrol C, Flemington E. $G_0/G_1$ growth arrest mediated by a region encompassing the basic leucine zipper (bZIP) domain of the Epstein-Barr virus transactivator Zta. J Biol Chem 1996; 271:31799-802.
17. Rodriguez A, Jung EJ, Yin Q, Cayrol C, Flemington EK. Role of c-myc regulation in Zta-mediated induction of the cyclin-dependent kinase inhibitors p21 and p27 and cell growth arrest. Virology 2001; 284:159-69.
18. Chang SS, Lo YC, Chua HH, Chiu HY, Tsai SC, Chen JY, et al. Critical role of p53 in histone deacetylase inhibitor-induced Epstein-Barr virus Zta expression. J Virol 2008; 82:7745-51.

19. Sato Y, Shirata N, Kudoh A, Iwahori S, Nakayama S, Murata T, et al. Expression of Epstein-Barr virus BZLF1 immediate-early protein induces p53 degradation independent of MDM2, leading to repression of p53-mediated transcription. Virology 2009; 388:204-11.
20. el-Deiry WS, Harper JW, O'Connor PM, Velculescu VE, Canman CE, Jackman J, et al. WAF1/CIP1 is induced in p53-mediated $G_1$ arrest and apoptosis. Cancer Res 1994; 54:1169-74.
21. Mauser A, Holley-Guthrie E, Simpson D, Kaufmann W, Kenney S. The Epstein-Barr virus immediate-early protein BZLF1 induces both a G(2) and a mitotic block. J Virol 2002; 76:10030-7.
22. Jayaraman L, Murthy KG, Zhu C, Curran T, Xanthoudakis S, Prives C. Identification of redox/repair protein Ref-1 as a potent activator of p53. Genes Dev 1997; 11:558-70.
23. Nie Y, Li HH, Bula CM, Liu X. Stimulation of p53 DNA binding by c-Abl requires the p53 C terminus and tetramerization. Mol Cell Biol 2000; 20:741-8.
24. Chen X, Farmer G, Zhu H, Prywes R, Prives C. Cooperative DNA binding of p53 with TFIID (TBP): a possible mechanism for transcriptional activation. Genes Dev 1993; 7:1837-49.
25. Zhang Q, Gutsch D, Kenney S. Functional and physical interaction between p53 and BZLF1: implications for Epstein-Barr virus latency. Mol Cell Biol 1994; 14:1929-38.
26. Wang S, El-Deiry WS. p73 or p53 directly regulates human p53 transcription to maintain cell cycle checkpoints. Cancer Res 2006; 66:6982-9.
27. Benoit V, Hellin AC, Huygen S, Gielen J, Bours V, Merville MP. Additive effect between NFkappaB subunits and p53 protein for transcriptional activation of human p53 promoter. Oncogene 2000; 19:4787-94.
28. Deffie A, Wu H, Reinke V, Lozano G. The tumor suppressor p53 regulates its own transcription. Mol Cell Biol 1993; 13:3415-23.
29. Mauser A, Saito S, Appella E, Anderson CW, Seaman WT, Kenney S. The Epstein-Barr virus immediate-early protein BZLF1 regulates p53 function through multiple mechanisms. J Virol 2002; 76:12503-12.
30. Wu FY, Chen H, Wang SE, ApRhys CM, Liao G, Fujimuro M, et al. CCAAT/enhancer binding protein alpha interacts with ZTA and mediates ZTA-induced p21(CIP-1) accumulation and G(1) cell cycle arrest during the Epstein-Barr virus lytic cycle. J Virol 2003; 77:1481-500.
31. Rodriguez A, Armstrong M, Dwyer D, Flemington E. Genetic dissection of cell growth arrest functions mediated by the Epstein-Barr virus lytic gene product, Zta. J Virol 1999; 73:9029-38.
32. Kudoh A, Fujita M, Kiyono T, Kuzushima K, Sugaya Y, Izuta S, et al. Reactivation of lytic replication from B cells latently infected with Epstein-Barr virus occurs with high S-phase cyclin-dependent kinase activity while inhibiting cellular DNA replication. J Virol 2003; 77:851-61.
33. Casavant NC, Luo MH, Rosenke K, Winegardner T, Zurawska A, Fortunato EA. Potential role for p53 in the permissive life cycle of human cytomegalovirus. J Virol 2006; 80:8390-401.
34. Jault FM, Jault JM, Ruchti F, Fortunato EA, Clark C, Corbeil J, et al. Cytomegalovirus infection induces high levels of cyclins, phosphorylated Rb and p53, leading to cell cycle arrest. J Virol 1995; 69:6697-704.
35. Rosenke K, Samuel MA, McDowell ET, Toerne MA, Fortunato EA. An intact sequence-specific DNA-binding domain is required for human cytomegalovirus-mediated sequestration of p53 and may promote in vivo binding to the viral genome during infection. Virology 2006; 348:19-34.
36. Daikoku T, Kudoh A, Fujita M, Sugaya Y, Isomura H, Shirata N, et al. Architecture of replication compartments formed during Epstein-Barr virus lytic replication. J Virol 2005; 79:3409-18.
37. Shieh SY, Ikeda M, Taya Y, Prives C. DNA damage-induced phosphorylation of p53 alleviates inhibition by MDM2. Cell 1997; 91:325-34.
38. Hsu CH, Chang MD, Tai KY, Yang YT, Wang PS, Chen CJ, et al. HCMV IE2-mediated inhibition of HAT activity downregulates p53 function. EMBO J 2004; 23:2269-80.
39. Sato Y, Miyake K, Kaneoka H, Iijima S. Sumoylation of CCAAT/enhancer-binding protein alpha and its functional roles in hepatocyte differentiation. J Biol Chem 2006; 281:21629-39.

*Journal of General Virology* (2010), **91**, 42–50 DOI 10.1099/vir.0.013482-0

# Quantitative analysis of Epstein–Barr virus (EBV)-related gene expression in patients with chronic active EBV infection

Seiko Iwata,[1] Kaoru Wada,[1] Satomi Tobita,[1] Kensei Gotoh,[2] Yoshinori Ito,[2] Ayako Demachi-Okamura,[3] Norio Shimizu,[4] Yukihiro Nishiyama[1] and Hiroshi Kimura[1]

Correspondence
Hiroshi Kimura
hkimura@med.nagoya-u.ac.jp

[1]Department of Virology, Nagoya University Graduate School of Medicine, Nagoya, Japan
[2]Department of Pediatrics, Nagoya University Graduate School of Medicine, Nagoya, Japan
[3]Division of Immunology, Aichi Cancer Center Research Institute, Nagoya, Japan
[4]Department of Virology, Division of Medical Science, Medical Research Institute, Graduate School of Medicine, Tokyo Medical and Dental University, Tokyo, Japan

Chronic active Epstein–Barr virus (CAEBV) infection is a systemic Epstein–Barr virus (EBV)-positive lymphoproliferative disorder characterized by persistent or recurrent infectious mononucleosis-like symptoms in patients with no known immunodeficiency. The detailed pathogenesis of the disease is unknown and no standard treatment regimen has been developed. EBV gene expression was analysed in peripheral blood samples collected from 24 patients with CAEBV infection. The expression levels of six latent and two lytic EBV genes were quantified by real-time RT-PCR. EBV-encoded small RNA 1 and *Bam*HI-A rightward transcripts were abundantly detected in all patients, and latent membrane protein (LMP) 2 was observed in most patients. EBV nuclear antigen (EBNA) 1 and LMP1 were detected less frequently and were expressed at lower levels. EBNA2 and the two lytic genes were not detected in any of the patients. The pattern of latent gene expression was determined to be latency type II. EBNA1 was detected more frequently and at higher levels in the clinically active patients. Quantifying EBV gene expression is useful in clarifying the pathogenesis of CAEBV infection and may provide information regarding a patient's disease prognosis, as well as possible therapeutic interventions.

Received 22 May 2009
Accepted 25 September 2009

## INTRODUCTION

Epstein–Barr virus (EBV) is the causative agent of infectious mononucleosis and is associated with several malignancies, including Burkitt's lymphoma, Hodgkin's lymphoma, nasopharyngeal carcinoma and post-transplant lymphoproliferative disorders (Cohen, 2000; Rickinson & Kieff, 2007; Williams & Crawford, 2006). Chronic active EBV (CAEBV) infection is a systemic EBV-positive lymphoproliferative disorder characterized by persistent or recurrent infectious mononucleosis-like symptoms in patients with no known immunodeficiency (Kimura, 2006; Okano *et al.*, 2005; Straus, 1988; Tosato *et al.*, 1985). The clonal expansion of EBV-infected T cells or natural killer (NK) cells plays a pathogenic role in patients with CAEBV, particularly among those in east Asia or central America (Kanegane *et al.*, 2002; Kimura, 2006; Quintanilla-Martinez *et al.*, 2000). These patients can be classified into two groups based on the predominantly infected cell type, T cells or NK cells (Kimura *et al.*, 2001, 2003). Nonetheless, the detailed pathogenesis of CAEBV remains elusive and no standard treatment regimen has been developed. Recently, haematopoietic stem cell transplantation (HSCT) was introduced as a curative therapy for CAEBV (Fujii *et al.*, 2000; Okamura *et al.*, 2000; Taketani *et al.*, 2002); however, transplant-related complications are common in such patients (Gotoh *et al.*, 2008; Kimura *et al.*, 2001, 2003). Alternatively, the EBV-related antigens expressed by infected cells are possible targets for treatment with EBV-specific cytotoxic T lymphocytes (CTLs) (Heslop *et al.*, 1996; Rooney *et al.*, 1998).

Viral gene expression in EBV-associated diseases is classified into one of three latency patterns (Cohen, 2000; Kieff & Rickinson, 2007). Latency type I, which is found in Burkitt's lymphoma, is characterized by EBV nuclear antigen (EBNA) 1, EBV-encoded small RNAs (EBERs) and *Bam*HI-A rightward transcripts (BARTs) expression (Tao *et al.*, 1998). In latency type II, which is characteristic

A supplementary table of primer sequences is available with the online version of this paper.

of Hodgkin's lymphoma and nasopharyngeal carcinoma, EBNA1, latent membrane protein (LMP) 1, LMP2, EBERs and BARTs are expressed (Brooks *et al.*, 1992; Deacon *et al.*, 1993). In latency type III, which is associated with post-transplant lymphoproliferative disorders, all of the above latent genes (EBNA1, EBNA2, EBNA3A, 3B, 3C, EBNA-LP, LMP1, LMP2, EBERs and BARTs) are expressed (Young *et al.*, 1989).

We recently reported that EBV gene expression could be quantitatively assessed by multiplex real-time RT-PCR (Kubota *et al.*, 2008). This method not only helps quantify EBV gene expression but also can be used to clarify the pathogenesis of EBV-associated diseases and to provide information about their prognosis and possible therapeutic interventions. Thus, in this study, we quantified the expression of six latent (EBNA1, EBNA2, LMP1, LMP2, EBER1 and BARTs) and two lytic [BZLF1 and glycoprotein (gp) 350/220] EBV genes in the peripheral blood of patients with CAEBV.

## RESULTS

First, we quantified the expression of several EBV genes in B, T and NK cell lines by real-time RT-PCR (Fig. 1a). In the EBV-positive B cell lines (Raji, LCL-1 and LCL-2), all six latent genes (EBNA1, EBNA2, LMP1, LMP2, EBER1 and BARTs) were detected, and the gene expression pattern was consistent with latency type III. Both lytic genes were detected in LCL-1 and -2 cells. However, none of the target genes was detected in BJAB, an EBV-negative cell line. EBNA1, LMP1, LMP2, EBER1 and BARTs, but not EBNA2, were detected in both the T (SNT-8, -13, -15 and -16) and NK cell lines (SNK-1, -6, -10 and KAI-3). The pattern of expression in the T and NK cell lines was latency type II.

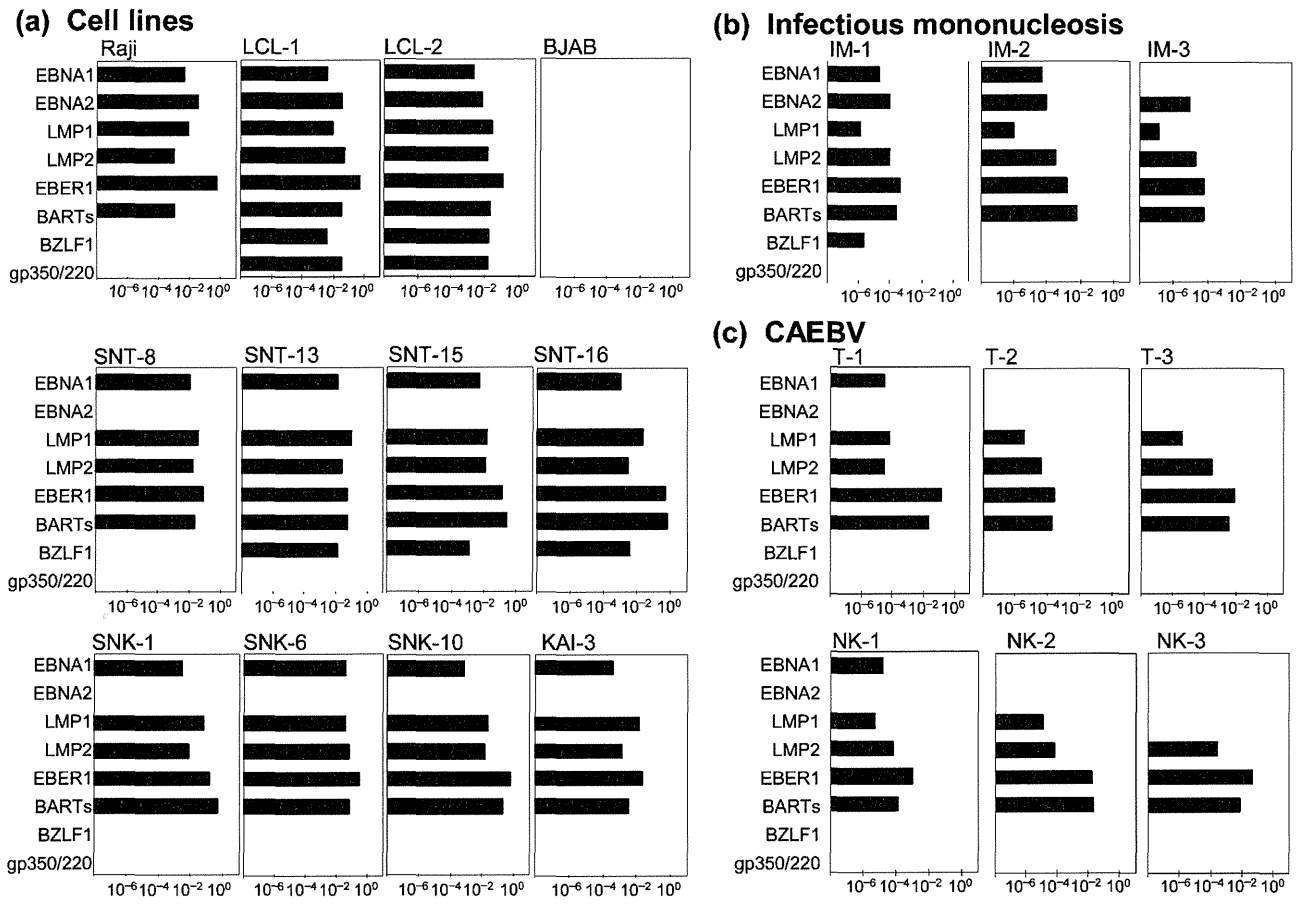


**Fig. 1.** Analysis of EBV gene expression by real-time RT-PCR. $\beta$2-Microglobin ($\beta$2 m) was used as an endogenous control and reference gene for relative quantification and was assigned an arbitrary value of 1 ($10^0$). (a) The quantity of each EBV gene in B, T and NK cells. Raji, LCL-1 and LCL-2 are EBV-positive B cell lines. BJAB is an EBV-negative B cell line. SNT-8, -13, -15 and -16 are EBV-positive T cell lines. SNK-1, -6, -10 and KAI-3 are EBV-positive NK cell lines. (b) Quantitative expression of the EBV genes in patients with infectious mononucleosis. (c) Representative results showing the relative expression of EBV genes in patients with a CAEBV infection. T-1, -2 and -3 are T-cell-type cases (patients 6, 9 and 11 in Table 1), while NK-1, -2 and -3 are NK-cell-type cases (patients 14, 15 and 19 in Table 1).

BZLF1 was detected in three of four T-cell lines, while gp350/220 was not detected in any of the cell lines, indicating an abortive lytic cycle. These results are consistent with those from previous reports (Leenman *et al.*, 2004; Tao *et al.*, 1998; Tsuge *et al.*, 1999; Zhang *et al.*, 2003), indicating the reliability of our system. We evaluated the sensitivity for each latent EBV gene using a cell mixture containing $1 \times 10^6$ EBV-negative BJAB cells and 10-fold serial dilutions of LCL-1 with latency III. The detection limits for EBNA1, EBNA2, LMP1, LMP2, EBER1 and BARTs were 0.1, 0.1, 0.01, 0.01, 0.001 and 0.01 % of LCL-1 cells, respectively. To evaluate the sensitivity for lytic genes, cell mixtures containing BJAB and Akata cells with a lytic infection, induced by human immunoglobulin G, were used. The detection limits for BZLF1 and gp350/220 were 0.1 % of Akata cells.

Next, we analysed blood from three patients with acute-phase infectious mononucleosis (Fig. 1b). EBNA2, LMP1, LMP2, EBER1 and BARTs were detected in the PBMCs of the patients, whereas EBNA1 was detected in two patients. The gene expression pattern in each case was latency type III. BZLF1 was detected in one patient, whereas gp350/220 was not detected in any patient. Furthermore, we analysed the PBMCs of 23 healthy carriers. Four healthy carriers were positive for EBV DNA. Real-time RT-PCR detected EBER1 and BARTs in the PBMCs of one carrier, while EBER1 alone was detected in a single additional carrier.

We next quantified the expression level of each gene in 24 patients with CAEBV. PBMCs collected at the time of diagnosis or referral were used in the analysis. The expression profiles of each patient are shown in Table 1, while the positive rates for each EBV gene are summarized in Table 2. EBER1 and BARTs were detected in each patient, while LMP2 was detected in most patients. EBNA1 and LMP1 were detected less frequently compared with EBER1 and BARTs ($P<0.0001$ and $P=0.004$, respectively). EBNA2 and the lytic genes BZLF1 and gp350/220 were undetected in all of the patients. Representative

**Table 1.** Characteristics and EBV gene expression profiles of 24 patients with chronic active EBV infection

ND, Not done. EBNA2, BZLF1 and gp350/220 were not expressed in any samples. EBER1 and BARTs were expressed in all samples.

| Patient | Age (years) | Gender | Cell type infected | Viral load* | | | | Disease type† | HSCT | Outcome | Viral load‡ | EBV gene expression | | |
|---|---|---|---|---|---|---|---|---|---|---|---|---|---|---|
| | | | | PBMC | $CD3^+$ | $CD19^+$ | $CD56^+$ | | | | | EBNA1 | LMP1 | LMP2 |
| 1 | 6 | M | T | 85925 | **157196** | 32828 | 62047 | I | − | Alive | 241000 | − | + | + |
| 2 | 5 | M | T | 74915 | **119024** | 12292 | **77651** | I | − | Alive | 392203 | + | − | + |
| 3 | 25 | M | T | 10749 | **12106** | 2742 | 5739 | I | − | Alive | 297 | − | − | − |
| 4 | 10 | M | T | 18308 | **23422** | 12665 | **27106** | I | − | Alive | 19363 | − | + | + |
| 5 | 6 | M | T | 14162 | **22559** | 1583 | 1073 | A | + | Alive | 14162 | − | − | + |
| 6 | 4 | F | T | 15776 | **17312** | 5243 | 4321 | A | + | Alive | 15776 | + | + | + |
| 7 | 11 | M | T | 60097 | **143852** | 23212 | 6352 | A | + | Alive | 60097 | − | − | + |
| 8 | 18 | F | T/B | 93458 | **118026** | **174042** | **267078** | A | + | Alive | 392734 | + | + | + |
| 9 | 14 | F | T | 30633 | **32730** | 8345 | 4760 | I | + | Alive | 30633 | − | + | + |
| 10 | 24 | F | T | 8589 | **43469** | 2388 | **12555** | A | − | Dead | 37148 | + | − | + |
| 11 | 23 | F | T | 5684 | **7990** | 4200 | 250 | I | + | Dead | 2764 | − | + | + |
| 12 | 13 | M | T | 3176 | **3579** | 948 | 839 | I | + | Dead | 10681 | + | + | + |
| 13 | 16 | F | T | 52978 | **55431** | 37536 | **84110** | I | + | Dead | 52978 | − | + | + |
| 14 | 11 | M | NK | 370000 | 31600 | 100000 | **1800000** | I | − | Alive | 339589 | + | + | + |
| 15 | 9 | M | NK | 77884 | 7428 | 17083 | **89352** | I | − | Alive | 89930 | − | + | + |
| 16 | 4 | M | NK | 74550 | 11288 | 18423 | **86361** | A | + | Alive | 74550 | + | + | + |
| 17 | 5 | F | NK | 11200 | 330 | 3300 | **23400** | A | + | Alive | 1108 | + | + | + |
| 18 | 3 | M | NK | 131957 | 1591 | 16450 | **917500** | I | + | Alive | 131957 | − | + | + |
| 19 | 9 | M | NK | 263429 | 92057 | 206565 | **425956** | I | + | Alive | 263429 | − | − | + |
| 20§ | 26 | F | NK | 18889 | ND | ND | ND | I | + | Alive | 18889 | − | + | − |
| 21 | 14 | F | NK | 1559 | 53 | 105 | **4302** | A | − | Dead | 1051 | − | − | − |
| 22 | 14 | F | NK | 20126 | 3288 | 1866 | **35252** | I | + | Dead | 44750 | + | + | + |
| 23§ | 16 | M | NK | 69121 | ND | ND | ND | I | + | Dead | 69121 | + | + | + |
| 24§ | 14 | F | NK | 1041 | ND | ND | ND | I | + | Dead | 1041 | − | − | − |

*Bold type indicates that EBV DNA was concentrated by fractionation; copies $(\mu g\ DNA)^{-1}$.

†Patients with severe symptoms were defined as having a clinically active disease (A); patients with no symptoms or with only skin symptoms were defined as having an inactive disease (I).

‡Indicates the EBV DNA in the PBMCs used for real-time RT-PCR analysis; copies $(\mu g\ DNA)^{-1}$.

§Infection was confirmed by *in situ* hybridization with EBER using fractionated cells.

**Table 2.** Detection of eight EBV-related genes in 24 patients with a CAEBV infection

| Gene | No. positive patients (%) | *P*-value* |
|---|---|---|
| EBNA1 | 10 (42) | <0.001 |
| EBNA2 | 0 (0) | <0.001 |
| LMP1 | 16 (67) | 0.004 |
| LMP2 | 20 (83) | 0.11 |
| EBER1 | 24 (100) | – |
| BARTs | 24 (100) | – |
| BZLF1 | 0 (0) | <0.001 |
| gp350/220 | 0 (0) | <0.001 |

*Comparison with EBER1 and BARTs. All *P*-values were obtained using Fisher's exact test.

quantitative results for each EBV gene are shown in Fig. 1(c).

The negative results obtained for EBNA1 and LMP1 raise the possibility that the test was not sensitive enough to detect low levels of expression. Therefore, we examined the correlation between the relative expression level for each gene and the EBV DNA load in the PBMCs (Fig. 2). For all of the EBV genes examined, the expression level correlated with the EBV DNA load. However, the samples with a low EBV DNA load were not always negative for EBNA1; similar findings were seen for LMP1.

To confirm the EBV gene expression profiles in various cell populations, we separated $CD3^+$, $CD19^+$ and $CD56^+$ cells from the PBMCs by immunomagnetic sorting and quantified the gene expression in each population by real-time RT-PCR using selected patients and healthy carriers. In one patient with T-cell-type CAEBV (patient 2 in Table 1; $CD3^+$ $CD56^+$ T cells harboured EBV), type II latent genes, such as EBNA1, LMP2, EBER1 and BARTs, were detected in both the $CD3^+$ and $CD56^+$ cell populations (Fig. 3a). In a patient with NK-cell-type CAEBV (patient 14 in Table 1), type II latent genes were detected primarily in the $CD56^+$ population (Fig. 3b). On the other hand, in a healthy carrier, EBER1 and BARTs were detected in the $CD19^+$ population (presumed to be the B-cell fraction; Fig. 3c). Importantly, the gene expression profiles in the mainly infected cells largely corresponded to those in the unsorted PBMCs in all three cases, suggesting that our PBMC data could be applied to the cells in the mainly infected population.

We next estimated the mean expression level for each EBV gene in 24 patients with CAEBV (Fig. 4a). EBER1 had the highest relative expression level, followed by BARTs, LMP2 and EBNA1, whereas LMP1 had the lowest. Next, we compared the expression level for each EBV gene between the T- and NK-cell types of CAEBV (Fig. 4b). No significant difference was found, although LMP2 expression tended to be higher in the T-cell type ($P$=0.09). We also compared the expression levels between the clinically active patients, who presented with severe symptoms at the time of sample collection, and clinically inactive patients (Fig. 4c). EBNA1 expression was 8.3 times higher in the active patients than in the inactive patients ($P$=0.02). Additionally, the rate of EBNA1-positive patients in the active group was significantly higher (75 versus 25 %; $P$=0.03). On the other hand, there was no difference in EBV DNA load in the peripheral blood between the active and inactive groups [$10^{4.4}$ versus $10^{4.5}$ copies (μg DNA)$^{-1}$; $P$=0.85]. We also investigated whether EBV gene expression at the time of diagnosis or referral to our hospital was associated with the subsequent disease outcome. We divided the patients into three groups: survivors without HSCT, survivors with HSCT and non-survivors. No significant difference was observed in the gene expression profiles of the three groups (Fig. 4d).

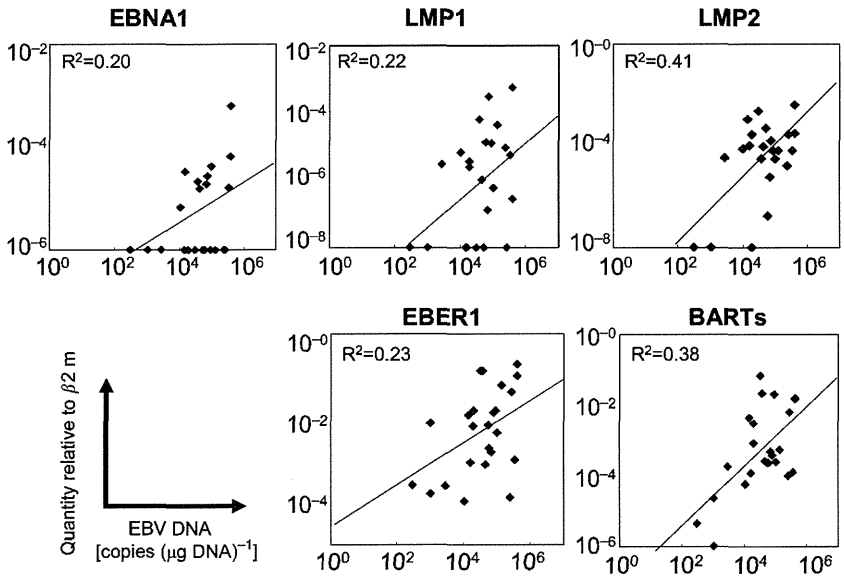


**Fig. 2.** Relationship between the quantity of each EBV gene and the EBV DNA load in PBMCs from patients with CAEBV. The correlation in all of these was statistically significant.

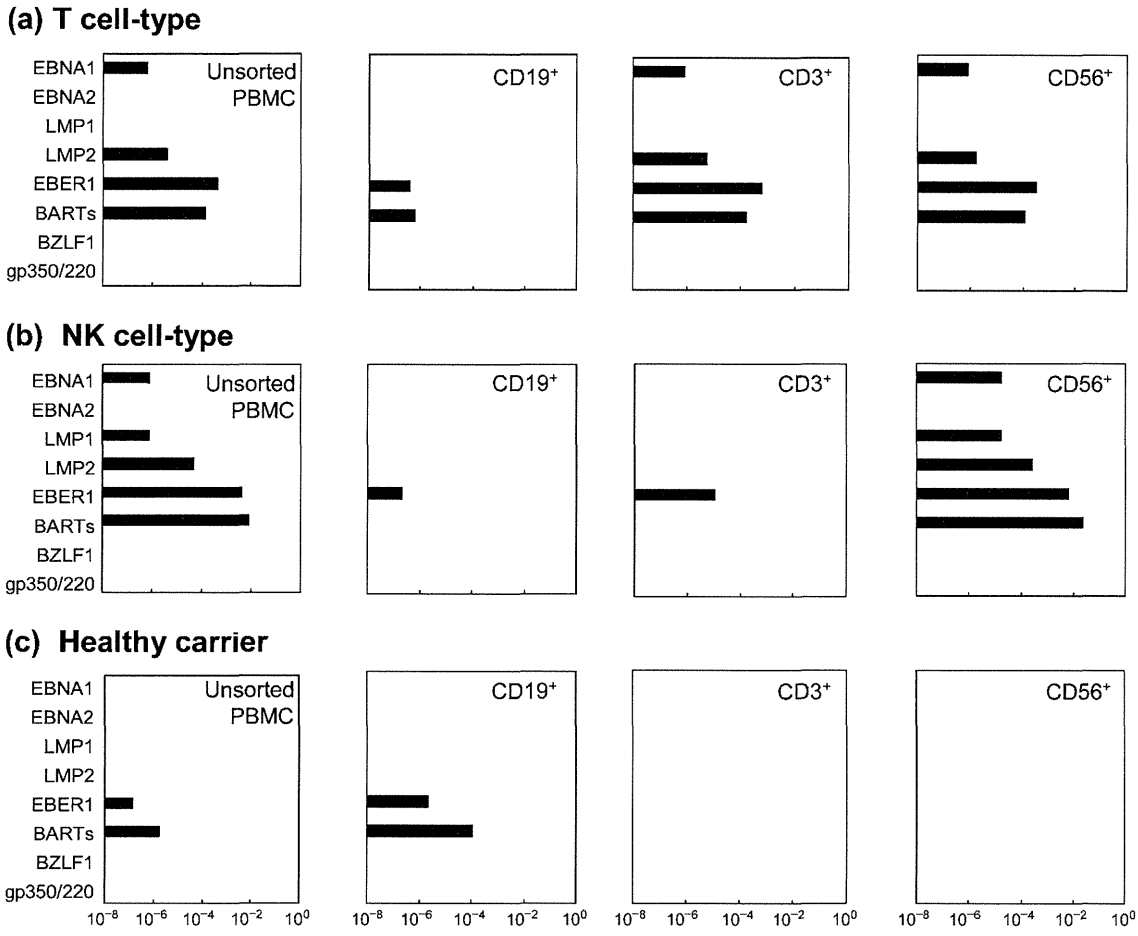


**Fig. 3.** EBV gene expression in sorted cell populations. CD19$^+$, CD3$^+$ and CD56$^+$ cells were separated by immunomagnetic sorting and analysed by real-time RT-PCR; unsorted PBMCs were analysed. (a) A T-cell-type CAEBV patient (patient 2 in Table 1; CD3$^+$ CD56$^+$ T cells were the main type of infected cells). (b) An NK-cell-type CAEBV patient (patient 14 in Table 1). (c) A healthy carrier whose PBMCs were positive for EBV DNA.

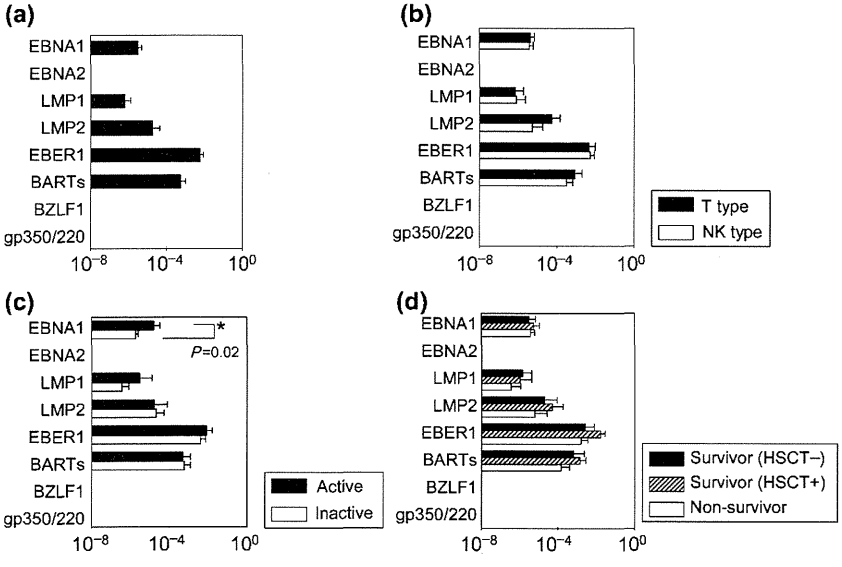


**Fig. 4.** EBV gene expression profile for patients with CAEBV. The quantity of each EBV gene was analysed by real-time RT-PCR and compared with the $\beta$2 m level; the mean ± SE (boxes and bars) was calculated for each gene. (a) Average expression of EBV genes in 24 patients with CAEBV. (b) Comparison between T- (13 cases) and NK- (11 cases) cell-types. (c) Comparison between clinically active (8 cases) and inactive (16 cases) patients. (d) Comparisons of surviving patients without HSCT (6 cases), surviving patients with HSCT (10 cases) and non-surviving patients (8 cases). The Mann–Whitney *U*-test was used to compare the expression values between the groups, while the analysis of variance was used to compare the groups of three.

Finally, to eliminate any potential influence of therapeutic interventions, we excluded six patients who had received therapy before entering our hospital and re-evaluated the expression of each gene in the remaining 18 patients. The level of EBNA1 expression in the active patients was 8.2 times higher than that in the inactive patients ($P$=0.03) and the rate of EBNA1-positive patients was significantly higher in the active group (83 versus 25 %; $P$=0.04). We also re-evaluated the disease outcome in these 18 patients. No significant difference was observed in the gene expression profiles between the three groups according to outcome (data not shown).

## DISCUSSION

Analysing the expression profile of EBV-related genes is essential to clarify the pathogenesis of EBV-associated diseases and to uncover information regarding the prognosis of individual patients and potential therapeutic interventions. In recent years, a quantitative method for the analysis of EBV gene expression has been applied to infectious mononucleosis (Weinberger *et al.*, 2004), Burkitt's lymphoma and nasopharyngeal carcinoma (Bell *et al.*, 2006). In the present study, we quantified the expression of six latent genes and two lytic genes in 24 patients with CAEBV using one-step multiplex real-time RT-PCR. To our knowledge, this is the first study to quantify EBV gene expression in CAEBV patients. EBNA1, LMP1, LMP2, EBER1 and BARTs were detected in the patient samples, whereas EBNA2 and the two lytic genes were not detected. The gene expression pattern was latency type II, consistent with previous qualitative RT-PCR results (Kimura *et al.*, 2005). Because the lytic genes BZLF1 and gp350/220 were undetected, a lytic infection is unlikely in the peripheral blood of the CAEBV patients. EBER1 and BARTs were detected in abundance in all patients, while LMP2 was found in most patients. EBNA1 and LMP1 were less frequently detected and had lower expression levels than EBER1 and BARTs. These results are in contrast with similar analyses using T or NK cell lines, in which EBNA1, LMP1, LMP2, EBER1 and BARTs were abundantly and comparably expressed. EBNA1, EBNA2 and EBNA3C are the dominant targets of $CD4^+$ T-cell responses, while EBNA3A, EBNA3B and EBNA3C are the dominant targets of $CD8^+$ T-cell responses (Hislop *et al.*, 2007). In those patients with CAEBV, most or all of these antigens were not expressed, contributing to the evasion of cellular immunity. The decreased frequency and low expression level of EBNA1 may also contribute to the immunological escape mechanism of CAEBV.

The expression profile identified in this study may be useful for obtaining information regarding potential immunotherapies. The EBV-related antigens expressed by infected cells are possible targets for treatment with EBV-specific CTLs. Several studies have reported the use of such therapies for CAEBV, but most have shown only limited effectiveness (Hagihara *et al.*, 2003; Kuzushima *et al.*, 1996; Savoldo *et al.*, 2002). These studies used EBV-specific CTLs that were generated from LCL and targeted latency type III antigens. Our results indicate that EBER1 and BARTs were the most frequently and abundantly expressed EBV genes, followed by LMP2. Because very little EBER1 and BARTs mRNA is translated into protein (Arrand & Rymo, 1982; Kieff & Rickinson, 2007), LMP2 would be the most favourable target for CTL therapy against CAEBV. Recently, EBV-specific CTLs targeted against LMP2 were used to treat Hodgkin's lymphoma and nasopharyngeal carcinoma, both of which are latency type II infections (Bollard *et al.*, 2004, 2007; Straathof *et al.*, 2005). Furthermore, patients with CAEBV generally lack LMP2-specific CTLs (Sugaya *et al.*, 2004). However, to develop effective and useful forms of immunotherapy, additional studies focusing on the nature of the infected cells and the underlying pathology of CAEBV are necessary.

In this study, we quantified the relative expression of EBV latent and lytic genes by real-time RT-PCR. There are a few drawbacks to our system. Firstly, we used $\beta$2-microglobulin ($\beta$2 m) as a reference for relative quantification; however, comparisons of the levels of expression between different genes may be compromised by variations in the efficiency of the primers used. Another option for such quantification is preparing a standard curve for each cDNA by diluting the plasmid and estimating the number of RNA copies to quantify the expression of each gene more accurately. Secondly, we determined the type of latency based on the patterns of viral gene expression. Promoter usage for EBNA1 is different between latency types I/II and III (Qp versus Cp) (Kieff & Rickinson, 2007). Primers capable of distinguishing between the two EBNA1 promoters would enable us to confirm the type of latency more accurately. Bell *et al.* (2006) used such a system to distinguish latency types and quantify gene expression using different EBNA1 primers.

There are several possible reasons why EBNA1 and LMP1 were detected less frequently in our analysis. First, EBV-infected T or NK cells in some patients with CAEBV may indeed express very little LMP1 or EBNA1. A previous experiment performed using nested RT-PCR, which is sensitive but not quantitative, showed that these genes were expressed in less than half of CAEBV patients (Kimura *et al.*, 2005). Second, the sensitivity of the test may be too low to detect these genes. However, those samples with a low EBV DNA load in this study were not always negative for EBNA1 or LMP1, indicating that low sensitivity was not the only reason that the expression of these genes was not detected. Moreover, EBV polymorphisms may have affected our results. Indeed, the primers used for LMP1 are specific for polymorphic regions (Kubota *et al.*, 2008). However, we used mixed primers for LMP1 to account for sequence variations, and the EBNA1 primers were designed to recognize fairly conserved regions. Furthermore, we also examined EBNA1- or LMP1-negative samples by nested RT-PCR using alternate primer sets (Kimura *et al.*, 2005).

Neither EBNA1 nor LMP1 was detected in any of the samples by nested PCR (data not shown).

EBNA1 was detected more frequently and abundantly in the clinically active patients. EBNA1 is the only EBV protein consistently expressed in all proliferating cells, and it plays central roles in the maintenance and replication of the episomal EBV genome. EBNA1 also has a role in cell growth and survival (Kieff & Rickinson, 2007; Thorley-Lawson & Gross, 2004). Recently, Saridakis *et al.* (2005) demonstrated that EBNA1 inhibits apoptosis by binding to USP7, which destabilizes p53. Together with our results, these findings suggest that EBNA1 plays an important part in the pathogenesis and symptoms of CAEBV.

EBV gene expression has been shown to be related to the prognosis of EBV-associated diseases. Kwon *et al.* (2006) evaluated EBER and LMP1 expression in patients with Hodgkin's lymphoma, while Tsang *et al.* (2003) reported a relationship between the recurrence and detection of LMP1 in patients with nasopharyngeal carcinoma. Similarly, we evaluated the relationship between EBV gene expression and the prognosis of CAEBV, but were unable to identify a significant link. Other factors that may have influenced the results of this study include the small sample size, short observation period and therapeutic interventions such as HSCT. Additional studies with a greater number of cases and a longer observation period are necessary to reach conclusions about the prognostic value of EBV gene quantification for CAEBV. In conclusion, we applied a real-time RT-PCR system to PBMCs from patients with CAEBV and identified the expression profiles of several EBV genes. Quantifying EBV gene expression may be useful in clarifying CAEBV pathogenesis and provide further information about therapeutic interventions, such as CTL therapy.

## METHODS

**Cell lines.** The EBV-positive B cell lines used in this study were Raji, Akata, lymphoblastoid cell line (LCL)-1 and LCL-2. BJAB, an EBV-negative B cell line, was used as a negative control. The EBV-positive T cell lines used were SNT-8, -13, -15 and -16 (Zhang *et al.*, 2003). The EBV-positive NK cell lines used were SNK-1, -6 and -10 (Zhang *et al.*, 2003) and KAI-3 (Tsuge *et al.*, 1999). The T/NK cell lines were derived from patients with CAEBV or nasal NK-/T-cell lymphomas.

**Patients.** Twenty-four patients (13 males and 11 females) with CAEBV, ranging in age from 3 to 26 years (median age 13 years), were enrolled in this study (Table 1). Each patient met the following diagnostic criteria: EBV-related symptoms for at least 6 months (e.g. fever, persistent hepatitis, extensive lymphadenopathy, hepatosplenomegaly, pancytopenia, uveitis, interstitial pneumonia, hydroa vacciniforme or hypersensitivity to mosquito bites), an increased EBV load in either the affected tissue or peripheral blood, and no evidence of previous immunological abnormalities or other recent infections that could explain the condition (Kimura, 2006; Kimura *et al.*, 2001). Based on the infected cell type, 13 patients were identified as having T-cell-type CAEBV, while 11 were identified as having NK-cell-type CAEBV. To determine which cells harboured the most EBV, peripheral blood mononuclear cells (PBMCs) were fractionated into $CD3^+$, $CD19^+$ and $CD56^+$ cells and analysed by either quantitative PCR or *in situ* hybridization, using EBER1 as a probe, as described previously (Kimura *et al.*, 2001, 2005). The patients were defined as having a T-cell-type infection if their $CD3^+$ cells contained larger amounts of EBV DNA than their PBMCs, or if their $CD3^+$ cells gave a positive hybridization signal with EBER1. The patients were defined as having an NK-cell-type infection if their $CD56^+$ cells, rather than their $CD3^+$ cells, were the major cells harbouring EBV. The EBV DNA copy numbers in each cell population are shown in Table 1.

Peripheral blood was collected at the time of diagnosis or referral to our hospital. Six of 24 patients had already received steroid therapy or chemotherapy. PBMCs were isolated using Ficoll–Paque density gradients (Pharmacia Biotech) and stored at −80 °C until further use. Eight patients with severe symptoms such as high fever, distinct hepatosplenomegaly, and/or elevated hepatic transaminase levels at the time of sample collection were defined as having clinically active disease, while 16 patients with no symptoms or with only skin symptoms, including hydroa vacciniforme, were defined as having inactive disease. Eight of the patients died after 1–49 months of observation (median 14 months). Sixteen of the patients, 10 of whom received HSCT, were alive after 9–115 months of observation (median 28 months). Twenty-three healthy carrier volunteers who were seropositive for EBV and three patients with infectious mononucleosis (aged 5, 11 and 29 years) were enrolled as controls.

Informed consent was obtained from all patients or their guardians. The institutional review board of Nagoya University Hospital approved the use of the specimens that were examined in this study.

**Real-time PCR assay.** DNA was extracted from $1 \times 10^6$ PBMCs using a QIAmp blood mini kit (Qiagen). EBV DNA was quantified by real-time PCR as described previously. The viral load is expressed as the number of copies $(\mu g\ DNA)^{-1}$ (Kimura *et al.*, 1999).

RNA was extracted from $1 \times 10^6$ cells using a QIAmp RNeasy mini kit (Qiagen). Contaminating DNA was removed by on-column DNase digestion using the RNase-free DNase set (Qiagen) (Kubota *et al.*, 2008). Viral mRNA expression was quantified by one-step multiplex real-time RT-PCR using an Mx3000P real-time PCR system (Stratagene) as described previously (Kubota *et al.*, 2008). All of the primer/probe combinations, except those for EBER1 lacking an intron, were designed to span introns to avoid amplifying residual genomic DNA. The primer and probe sequences are listed in Supplementary Table S1 (available in JGV Online). The primers used for EBNA1, EBNA2, LMP1 and BZLF1, which were described previously (Kubota *et al.*, 2008), were modified according to sequence variations amongst the strains. The stably expressed housekeeping gene $\beta 2$ m was used as an endogenous control and reference gene for relative quantification (Patel *et al.*, 2004).

**Cell sorting and gene expression analysis.** $CD3^+$, $CD19^+$ and $CD56^+$ cells were separated from $1 \times 10^7$ PBMCs by immunomagnetic sorting using anti-CD3, -CD19 and -CD56 MACS Microbeads, respectively (Miltenyi Biotec). After two rounds of sorting, the purity of the populations exceeded 95 %. RNA was extracted from each cell population for real-time RT-PCR analysis. For comparison, RNA was also extracted from unsorted PBMCs.

**Statistical analyses.** All statistical analyses were performed using StatView (version 5.0; SAS Institute). Geometric (logarithmic) means were calculated for the expression of each EBV gene. For the negative samples, the default value, which was defined as the lowest level of expression for a particular gene, was used for the calculation. The default values for the undetected genes EBNA1, LMP1 and LMP2 were $10^{-6}$, $10^{-8}$ and $10^{-8}$, respectively. The Mann–Whitney *U*-test was used to compare the expression levels between groups, while analysis of variance was used to compare three groups. Fisher's exact

test was used to compare positive rates of gene expression. A regression analysis was used to compare the expression of each gene and the EBV DNA load. *P*-values $<0.05$ were deemed to be statistically significant.

## ACKNOWLEDGEMENTS

We thank the following people for their contributions to this study: Kayoko Matsunaga (Fujita Health University); Masaki Ito, Atsushi Kikuta, and Mitsuaki Hosoya (Fukushima Medical University); Tomohiro Kinoshita (Nagoya University); Kazuhiko Shirota (National Hospital Organization Shizuoka Medical Center); Mariko Seishima (Ogaki Municipal Hispital); Masashi Shiomi (Osaka City General Hospital); Hajime Katsumata and Yasuo Horikoshi (Shizuoka Children's Hospital); Tsuyoshi Ito (Toyohashi City Hospital); and Sachiyo Kamimura (University of Miyazaki). This study was supported in part by a grant from the Ministry of Education, Culture, Sports, Science and Technology, Japan (19591247).

## REFERENCES

**Arrand, J. R. & Rymo, L. (1982).** Characterization of the major Epstein–Barr virus-specific RNA in Burkitt lymphoma-derived cells. *J Virol* **41**, 376–389.

**Bell, A. I., Groves, K., Kelly, G. L., Croom-Carter, D., Hui, E., Chan, A. T. & Rickinson, A. B. (2006).** Analysis of Epstein–Barr virus latent gene expression in endemic Burkitt's lymphoma and nasopharyngeal carcinoma tumour cells by using quantitative real-time PCR assays. *J Gen Virol* **87**, 2885–2890.

**Bollard, C. M., Aguilar, L., Straathof, K. C., Gahn, B., Huls, M. H., Rousseau, A., Sixbey, J., Gresik, M. V., Carrum, G. & other authors (2004).** Cytotoxic T lymphocyte therapy for Epstein–Barr virus$^+$ Hodgkin's disease. *J Exp Med* **200**, 1623–1633.

**Bollard, C. M., Gottschalk, S., Leen, A. M., Weiss, H., Straathof, K. C., Carrum, G., Khalil, M., Wu, M. F., Huls, M. H. & other authors (2007).** Complete responses of relapsed lymphoma following genetic modification of tumor-antigen presenting cells and T-lymphocyte transfer. *Blood* **110**, 2838–2845.

**Brooks, L., Yao, Q. Y., Rickinson, A. B. & Young, L. S. (1992).** Epstein–Barr virus latent gene transcription in nasopharyngeal carcinoma cells: coexpression of EBNA1, LMP1, and LMP2 transcripts. *J Virol* **66**, 2689–2697.

**Cohen, J. I. (2000).** Epstein–Barr virus infection. *N Engl J Med* **343**, 481–492.

**Deacon, E. M., Pallesen, G., Niedobitek, G., Crocker, J., Brooks, L., Rickinson, A. B. & Young, L. S. (1993).** Epstein–Barr virus and Hodgkin's disease: transcriptional analysis of virus latency in the malignant cells. *J Exp Med* **177**, 339–349.

**Fujii, N., Takenaka, K., Hiraki, A., Maeda, Y., Ikeda, K., Shinagawa, K., Ashiba, A., Munemasa, M., Sunami, K. & other authors (2000).** Allogeneic peripheral blood stem cell transplantation for the treatment of chronic active Epstein-Barr virus infection. *Bone Marrow Transplant* **26**, 805–808.

**Gotoh, K., Ito, Y., Shibata-Watanabe, Y., Kawada, J., Takahashi, Y., Yagasaki, H., Kojima, S., Nishiyama, Y. & Kimura, H. (2008).** Clinical and virological characteristics of 15 patients with chronic active Epstein–Barr virus infection treated with hematopoietic stem cell transplantation. *Clin Infect Dis* **46**, 1525–1534.

**Hagihara, M., Tsuchiya, T., Hyodo, O., Ueda, Y., Tazume, K., Masui, A., Kanemura, A., Yoshiba, F., Takashimizu, S. & other authors (2003).** Clinical effects of infusing anti-Epstein–Barr virus (EBV)-specific cytotoxic T-lymphocytes into patients with severe chronic active EBV infection. *Int J Hematol* **78**, 62–68.

**Heslop, H. E., Ng, C. Y., Li, C., Smith, C. A., Loftin, S. K., Krance, R. A., Brenner, M. K. & Rooney, C. M. (1996).** Long-term restoration of immunity against Epstein–Barr virus infection by adoptive transfer of gene-modified virus-specific T lymphocytes. *Nat Med* **2**, 551–555.

**Hislop, A. D., Taylor, G. S., Sauce, D. & Rickinson, A. B. (2007).** Cellular responses to viral infection in humans: lessons from Epstein–Barr virus. *Annu Rev Immunol* **25**, 587–617.

**Kanegane, H., Nomura, K., Miyawaki, T. & Tosato, G. (2002).** Biological aspects of Epstein–Barr virus (EBV)-infected lymphocytes in chronic active EBV infection and associated malignancies. *Crit Rev Oncol Hematol* **44**, 239–249.

**Kieff, E. D. & Rickinson, A. V. (2007).** Epstein–Barr virus and its replication. In *Fields Virology*, pp. 2603–2654. Edited by D. M. Knipe & P. M. Howley. Philadelphia: Lippincott Williams & Wilkins.

**Kimura, H. (2006).** Pathogenesis of chronic active Epstein–Barr virus infection: is this an infectious disease, lymphoproliferative disorder, or immunodeficiency? *Rev Med Virol* **16**, 251–261.

**Kimura, H., Morita, M., Yabuta, Y., Kuzushima, K., Kato, K., Kojima, S., Matsuyama, T. & Morishima, T. (1999).** Quantitative analysis of Epstein–Barr virus load by using a real-time PCR assay. *J Clin Microbiol* **37**, 132–136.

**Kimura, H., Hoshino, Y., Kanegane, H., Tsuge, I., Okamura, T., Kawa, K. & Morishima, T. (2001).** Clinical and virologic characteristics of chronic active Epstein-Barr virus infection. *Blood* **98**, 280–286.

**Kimura, H., Morishima, T., Kanegane, H., Ohga, S., Hoshino, Y., Maeda, A., Imai, S., Okano, M., Morio, T. & other authors (2003).** Prognostic factors for chronic active Epstein–Barr virus infection. *J Infect Dis* **187**, 527–533.

**Kimura, H., Hoshino, Y., Hara, S., Sugaya, N., Kawada, J., Shibata, Y., Kojima, S., Nagasaka, T., Kuzushima, K. & Morishima, T. (2005).** Differences between T cell-type and natural killer cell-type chronic active Epstein–Barr virus infection. *J Infect Dis* **191**, 531–539.

**Kubota, N., Wada, K., Ito, Y., Shimoyama, Y., Nakamura, S., Nishiyama, Y. & Kimura, H. (2008).** One-step multiplex real-time PCR assay to analyse the latency patterns of Epstein–Barr virus infection. *J Virol Methods* **147**, 26–36.

**Kuzushima, K., Yamamoto, M., Kimura, H., Ando, Y., Kudo, T., Tsuge, I. & Morishima, T. (1996).** Establishment of anti-Epstein–Barr virus (EBV) cellular immunity by adoptive transfer of virus-specific cytotoxic T lymphocytes from an HLA-matched sibling to a patient with severe chronic active EBV infection. *Clin Exp Immunol* **103**, 192–198.

**Kwon, J. M., Park, Y. H., Kang, J. H., Kim, K., Ko, Y. H., Ryoo, B. Y., Lee, S. S., Lee, S. I., Koo, H. H. & Kim, W. S. (2006).** The effect of Epstein–Barr virus status on clinical outcome in Hodgkin's lymphoma. *Ann Hematol* **85**, 463–468.

**Leenman, E. E., Panzer-Grumayer, R. E., Fischer, S., Leitch, H. A., Horsman, D. E., Lion, T., Gadner, H., Ambros, P. F. & Lestou, V. S. (2004).** Rapid determination of Epstein–Barr virus latent or lytic infection in single human cells using *in situ* hybridization. *Mod Pathol* **17**, 1564–1572.

**Okamura, T., Hatsukawa, Y., Arai, H., Inoue, M. & Kawa, K. (2000).** Blood stem-cell transplantation for chronic active Epstein–Barr virus with lymphoproliferation. *Lancet* **356**, 223–224.

**Okano, M., Kawa, K., Kimura, H., Yachie, A., Wakiguchi, H., Maeda, A., Imai, S., Ohga, S., Kanegane, H. & other authors (2005).** Proposed guidelines for diagnosing chronic active Epstein–Barr virus infection. *Am J Hematol* **80**, 64–69.

**Patel, K., Whelan, P. J., Prescott, S., Brownhill, S. C., Johnston, C. F., Selby, P. J. & Burchill, S. A. (2004).** The use of real-time reverse

transcription-PCR for prostate-specific antigen mRNA to discriminate between blood samples from healthy volunteers and from patients with metastatic prostate cancer. *Clin Cancer Res* **10**, 7511–7519.

**Quintanilla-Martinez, L., Kumar, S., Fend, F., Reyes, E., Teruya-Feldstein, J., Kingma, D. W., Sorbara, L., Raffeld, M., Straus, S. E. & Jaffe, E. S. (2000).** Fulminant EBV(+) T-cell lymphoproliferative disorder following acute/chronic EBV infection: a distinct clinicopathologic syndrome. *Blood* **96**, 443–451.

**Rickinson, A. B. & Kieff, E. (2007).** Epstein–Barr virus. In *Fields Virology*, pp. 2655–2700. Edited by D. M. Knipe & P. M. Howley. Philadelphia: Lippincott Williams & Wilkins.

**Rooney, C. M., Smith, C. A., Ng, C. Y., Loftin, S. K., Sixbey, J. W., Gan, Y., Srivastava, D. K., Bowman, L. C., Krance, R. A. & other authors (1998).** Infusion of cytotoxic T cells for the prevention and treatment of Epstein–Barr virus-induced lymphoma in allogeneic transplant recipients. *Blood* **92**, 1549–1555.

**Saridakis, V., Sheng, Y., Sarkari, F., Holowaty, M. N., Shire, K., Nguyen, T., Zhang, R. G., Liao, J., Lee, W. & other authors (2005).** Structure of the p53 binding domain of HAUSP/USP7 bound to Epstein–Barr nuclear antigen 1 implications for EBV-mediated immortalization. *Mol Cell* **18**, 25–36.

**Savoldo, B., Huls, M. H., Liu, Z., Okamura, T., Volk, H. D., Reinke, P., Sabat, R., Babel, N., Jones, J. F. & other authors (2002).** Autologous Epstein–Barr virus (EBV)-specific cytotoxic T cells for the treatment of persistent active EBV infection. *Blood* **100**, 4059–4066.

**Straathof, K. C., Leen, A. M., Buza, E. L., Taylor, G., Huls, M. H., Heslop, H. E., Rooney, C. M. & Bollard, C. M. (2005).** Characterization of latent membrane protein 2 specificity in CTL lines from patients with EBV-positive nasopharyngeal carcinoma and lymphoma. *J Immunol* **175**, 4137–4147.

**Straus, S. E. (1988).** The chronic mononucleosis syndrome. *J Infect Dis* **157**, 405–412.

**Sugaya, N., Kimura, H., Hara, S., Hoshino, Y., Kojima, S., Morishima, T., Tsurumi, T. & Kuzushima, K. (2004).** Quantitative analysis of Epstein–Barr virus (EBV)-specific $CD8^+$ T cells in patients with chronic active EBV infection. *J Infect Dis* **190**, 985–988.

**Taketani, T., Kikuchi, A., Inatomi, J., Hanada, R., Kawaguchi, H., Ida, K., Oh-Ishi, T., Arai, T., Kishimoto, H. & Yamamoto, K. (2002).** Chronic active Epstein–Barr virus infection (CAEBV) successfully treated with allogeneic peripheral blood stem cell transplantation. *Bone Marrow Transplant* **29**, 531–533.

**Tao, Q., Robertson, K. D., Manns, A., Hildesheim, A. & Ambinder, R. F. (1998).** Epstein–Barr virus (EBV) in endemic Burkitt's lymphoma: molecular analysis of primary tumor tissue. *Blood* **91**, 1373–1381.

**Thorley-Lawson, D. A. & Gross, A. (2004).** Persistence of the Epstein–Barr virus and the origins of associated lymphomas. *N Engl J Med* **350**, 1328–1337.

**Tosato, G., Straus, S., Henle, W., Pike, S. E. & Blaese, R. M. (1985).** Characteristic T cell dysfunction in patients with chronic active Epstein–Barr virus infection (chronic infectious mononucleosis). *J Immunol* **134**, 3082–3088.

**Tsang, N. M., Chuang, C. C., Tseng, C. K., Hao, S. P., Kuo, T. T., Lin, C. Y. & Pai, P. C. (2003).** Presence of the latent membrane protein 1 gene in nasopharyngeal swabs from patients with mucosal recurrent nasopharyngeal carcinoma. *Cancer* **98**, 2385–2392.

**Tsuge, I., Morishima, T., Morita, M., Kimura, H., Kuzushima, K. & Matsuoka, H. (1999).** Characterization of Epstein–Barr virus (EBV)-infected natural killer (NK) cell proliferation in patients with severe mosquito allergy; establishment of an IL-2-dependent NK-like cell line. *Clin Exp Immunol* **115**, 385–392.

**Weinberger, B., Plentz, A., Weinberger, K. M., Hahn, J., Holler, E. & Jilg, W. (2004).** Quantitation of Epstein–Barr virus mRNA using reverse transcription and real-time PCR. *J Med Virol* **74**, 612–618.

**Williams, H. & Crawford, D. H. (2006).** Epstein–Barr virus: the impact of scientific advances on clinical practice. *Blood* **107**, 862–869.

**Young, L., Alfieri, C., Hennessy, K., Evans, H., O'Hara, C., Anderson, K. C., Ritz, J., Shapiro, R. S., Rickinson, A. & other authors (1989).** Expression of Epstein–Barr virus transformation-associated genes in tissues of patients with EBV lymphoproliferative disease. *N Engl J Med* **321**, 1080–1085.

**Zhang, Y., Nagata, H., Ikeuchi, T., Mukai, H., Oyoshi, M. K., Demachi, A., Morio, T., Wakiguchi, H., Kimura, N. & other authors (2003).** Common cytological and cytogenetic features of Epstein–Barr virus (EBV)-positive natural killer (NK) cells and cell lines derived from patients with nasal T/NK-cell lymphomas, chronic active EBV infection and hydroa vacciniforme-like eruptions. *Br J Haematol* **121**, 805–814.

# Detection of EBV genomes in plasmablasts/plasma cells and non-B cells in the blood of most patients with EBV lymphoproliferative disorders by using Immuno-FISH

Sara Calattini,[1] Irini Sereti,[2] Philip Scheinberg,[3] Hiroshi Kimura,[4] Richard W. Childs,[3] and Jeffrey I. Cohen[1]

[1]Medical Virology Section, Laboratory of Infectious Diseases, [2]Laboratory of Immunoregulation, National Institute of Allergy and Infectious Diseases, and [3]Hematology Branch, National Heart Lung and Blood Institute, National Institutes of Health, Bethesda, MD; and [4]Department of Virology, Nagoya University Graduate School of Medicine, Nagoya, Japan

**Epstein-Barr virus (EBV) is present in B cells in the blood of healthy people; few studies have looked for EBV in other cell types in blood from patients with lymphoproliferative disorders. We use a new technique combining immunofluorescent cell-surface staining and fluorescent in situ hybridization to quantify both EBV copy number per cell and cell types in blood from patients with high EBV DNA loads. In addition to CD20$^+$ B cells, EBV was present in plasmablast/plasma cells in the blood of 50% of patients, in monocytes or T cells in a small proportion of patients, and in "non-B, non-T, non-monocytes" in 69% of patients. The mean EBV copy number in B cells was significantly higher than in plasmablast/plasma cells. There was no correlation between EBV load and virus copy number per cell. Although we detected CD21, the EBV B-cell receptor, on EBV-infected B cells, we could not detect it on virus-infected T cells. These findings expand the range of cell types infected in the blood. Determining the number of EBV genomes per cell and the type of cells infected in patients with high EBV loads may provide additional prognostic information for the development of EBV lymphoproliferative diseases. (*Blood.* 2010;116(22):4546-4559)**

## Introduction

Epstein-Barr virus (EBV) infects more than 90% of the human population.[1] In immunocompetent hosts, the virus is latent in B cells of the peripheral blood and is not associated with disease.[2-4] However, in immunocompromised patients, immune surveillance to the virus is often impaired, a larger number of B cells are infected with EBV, and the virus can contribute to lymphoproliferative disease. Approximately 1%-20% of transplant recipients can develop posttransplantation lymphoproliferative disease (PTLD) during the first year after transplantation, and approximately 90% of these cases are EBV positive.[5] Persons with AIDS have a 60-fold increased risk of developing lymphoma, compared with the general population, and virtually all Hodgkin and non-Hodgkin lymphomas that occur in the late stages of HIV infection are EBV positive.[6]

Although EBV establishes a latent infection in peripheral blood B cells of healthy people, less is known about the phenotype of virus-infected cells in the blood of immunocompromised persons with high EBV DNA loads. Most studies have focused on the phenotype of virus-infected B cells in transplant recipients.[2,7-11] However, EBV can infect cells other than B cells, including T cells, natural killer (NK) cells, monocytes, and pre-Langerhans cells.[12-16]

Several techniques have been developed to detect EBV in cells. In situ hybridization using a probe that detects the EBV-encoded RNAs (EBERs) is considered the best test for localizing latent EBV in tissue samples.[17] Combined staining for EBERs and antibodies to cell-surface markers for tissues on microscope slides, or for peripheral blood by flow cytometry,[18] has been used to determine the phenotype of the EBV-infected cells. Although detection of EBERs indicates that cells are infected with EBV, this test cannot provide an estimate of the number of EBV genomes present per cell.

We describe a new technique (Immuno-FISH) that combines immunofluorescent staining for surface proteins (using antibodies directly conjugated to fluorochromes) and fluorescent in situ hybridization for EBV DNA. This technique allows the simultaneous determination of the cell type infected by EBV and quantification of EBV copy number in the infected cell. We show that EBV is present not only in B cells, but also in a large percentage of other cell types in the peripheral blood of patients with high EBV DNA loads. In addition, we correlate the number of EBV genomes per cell with the phenotype of the infected cells.

## Methods

### Study participants

Patients had blood drawn after informed consent was obtained in accordance with the Declaration of Helsinki under protocols approved by the Institutional Review Boards of the National Institute of Allergy and Infectious Diseases, the National Cancer Institute, the National Heart, Lung, and Blood Institute (patients 1-23), Nagoya University Hospital (patients 24-27), or the University of Maryland and the National Institute of Allergy and Infectious Diseases (patients 28-29). For patients from the United States, we selected those whose EBV DNA loads were more than 5000 copies per million cells (normal is $< 200$ copies/million cells) and, for patients from Japan, more than 50 000 copies per $\mu$g of DNA.

Submitted May 14, 2010; accepted July 25, 2010. Prepublished online as *Blood* First Edition paper, August 10, 2010; DOI 10.1182/blood-2010-05-285452.

The online version of this article contains a data supplement.

The publication costs of this article were defrayed in part by page charge payment. Therefore, and solely to indicate this fact, this article is hereby marked "advertisement" in accordance with 18 USC section 1734.

### Measurement of EBV DNA in blood

For patients 1-23 and 28-29, the EBV DNA load data were reported as the number of EBV genomes per $10^6$ cells. Peripheral blood mononuclear cells (PBMCs) were lysed and EBV quantitative real-time polymerase chain reaction (qPCR) was performed as previously described[19] (see supplemental data, available on the *Blood* Web site; see the Supplemental Materials link at the top of the online article).

### Immuno-FISH procedure

Cryopreserved PBMCs were thawed at 37°C, washed once in media and once in phosphate-buffered saline (PBS), and then resuspended in a solution of 0.2N acetic acid, 0.02N HCl, in Tris HCl 0.1M (adjusted to pH 3.7) for 15 minutes at room temperature. The cells were washed twice in PBS and incubated with fluorochrome-conjugated monoclonal antibodies (to stain cell-surface proteins) in suspension for 30 minutes at 4°C. Cells were washed 2× with PBS and applied to Superfrost Plus microscope slides (Thermo Fisher Scientific) by cytospin centrifugation at 500*g* for 5 minutes.

The cells were then fixed with 5mM $BS_3$ (Thermo Fisher Scientific) for 30 minutes at room temperature and permeabilized with Triton X-100 (Sigma-Aldrich) at 0.5% in PBS for 10 minutes at room temperature. The slides were washed with PBS and incubated at 37°C for 1 hour in a solution of 2× saline-sodium citrate (SSC) containing 10 U/mL RNAse T1 (Roche Applied Science) and 15 U/mL RNAse A (Sigma-Aldrich). The slides were then washed once in 0.1M Tris-HCl (pH 7.5), incubated for 5 minutes in a solution of 0.1M Tris-HCl (pH 7.5)/0.1M glycine, and then washed in 2× SSC.

FISH was performed with a biotinylated EBV BioProbe (Enzo Life Sciences) specific for the BamHI W region of EBV. There are 5-12 BamH1 W repeats per EBV genome, depending on the virus strain.[20] The probe was diluted to a final concentration of 0.25 ng/μL in hybridization buffer (Enzo Life Sciences) and denatured at 94°C for 10 minutes. The slides were then incubated with the denatured probe at 85°C for 6 minutes under a coverslip sealed with rubber cement and then hybridized overnight at 37°C. Slides were washed 2× for 15 minutes in a solution of 0.1× SSC, 0.1% Tween, and 1% BSA at 42°C, washed once in 0.1× SSC, and washed 3 times in Tris-HCl (0.1M; pH 7.5). Slides were incubated with streptavidin-conjugated Alexa 488 or streptavidin-conjugated Alexa 594 for 15 minutes at a final concentration of 1 μg/mL, washed in PBS/Tween 0.1% for 5 minutes, washed 3× in Tris-HCl (0.1M; pH 7.5), and mounted with Fluoromount-G medium (Southern-Biotech). The slides were visualized with a Leica SP5 confocal microscope (Carl Zeiss), with a 63×/1.4 numerical aperture magnification objective. For each field, photographs of serial z-stack sections (0.5 μm thick) were obtained throughout the cells and then overlapped to quantify the total number of fluorescent spots (each spot corresponds to one EBV genome copy) in the cells.

When FISH alone was performed, the cells were incubated for 15 minutes with a solution of 0.2N acetic acid, 0.02N HCl, in Tris HCl (0.1M; adjusted to pH 3.7), then applied to the slides, fixed with BS3, permeabilized with Triton X-100, and FISH was performed as described above.

### Cell-surface markers, fluorochromes, and EBV antibodies

After incubation with acetic acid and HCl, cells were resuspended in PBS at a concentration of $1 \times 10^6$ cells per 100 μL and stained with mouse anti–human monoclonal antibodies to label cell-surface markers.

For the sorting procedure, the CD19 phycoerythrin (PE)–Cy7 antibody was used to identify B cells. The CD3 allophycocyanin (APC)–H7 and the CD56 APC antibodies were used to identify the T and NK subpopulations, respectively. All of these antibodies were purchased from BD Biosciences.

For each patient sample, cells were stained with different combinations of monoclonal antibodies. The first combination contained antibodies that recognize CD3 T cells (Alexa 594), B cells (Alexa 647), and monocytes (V450); the second combination included antibodies that recognize CD3 T cells (Alexa 594), NK cells (Alexa 647), and monocytes (V450), and the third combination contained antibodies that recognize the B-cell surface marker, CD20 (Alexa 488), together with the κ and λ light chains of immunoglobulin (Ig; Alexa 647). Staining with antibodies that recognize the κ and λ chains was performed after permeabilization of the cells to allow staining of intracytoplasmic immunoglobulin. The biotinylated FISH EBV probe was detected using streptavidin-conjugated Alexa 488 for the first and second combinations, and with streptavidin-conjugated Alexa 594 for the third combination.

For samples in which EBV was detected in CD3 T cells, another aliquot of cells was stained with Alexa 647–conjugated anti-CD4 antibody and Alexa 488–conjugated anti-CD8 antibody, and the FISH probe was detected using streptavidin-conjugated Alexa 594.

To detect lytic replication of EBV, PBMCs were stained with a combination of antibodies for B and T cells (CD3 Alexa 594 and CD19/CD20 Alexa 647), applied to Superfrost Plus microscope slides, and fixed and permeabilized as previously described. Cells were then incubated for 30 minutes with BZLF1 monoclonal antibody (Meridian Life Science) conjugated with Alexa 488. Slides were then washed 3× in PBS and mounted with Fluoromount-G medium. B95-8 and BJAB cells were stained with BZLF1 antibody as positive and negative controls for virus lytic replication, respectively.

## Results

### FISH and Immuno-FISH assays are sensitive and specific

To determine the sensitivity and specificity of our FISH assay, we diluted EBV-positive X50-7 cells with EBV-negative BJAB cells and performed FISH. A mixture of 10% of X50-7 cells and 90% BJAB cells yielded 9.6% (11/114) EBV-positive cells by FISH, whereas a mixture of 1% X50-7 cells and 99% BJAB cells showed 1.1% (8/745) EBV-positive cells by FISH (representative example in supplemental Figure S1A-B). As controls, one slide of 100% EBV-positive X50-7 cells and one of 100% EBV-negative BJAB cells were also stained by FISH, and EBV episomes were detected in all of the EBV-positive cells and none of the EBV-negative cells (supplemental Figure 1C-D). As an additional negative control, Immuno-FISH staining of cells from patients with very low or undetectable EBV viral loads by PCR did not detect any FISH-positive cells (data not shown). Combining Immuno-FISH with DAPI (4′,6′-diamidino-2-phenylindole) staining, we found EBV DNA only in the nucleus of the cells (data not shown). These results indicate that the FISH procedure is specific, and that it can detect at least 1% of EBV-positive cells in a mixture of EBV-negative cells.

We also quantified the number of EBV genomes per cell using the FISH procedure. EBV-positive cells were analyzed by confocal microscopy; serial z-stack sections were imaged every 0.5 μm, overlapped, and the number of fluorescent spots, each corresponding to a single EBV episome, was counted. Analysis of 65 individual X-50-7 cells from 5 separate experiments showed a median of 7 EBV genomes per cell, with a mean of 9.4 genomes per cell (range, 2-18 genomes per cell). These results are similar to those previously reported, indicating that X50-7 cells contain approximately 5 EBV genomes per cell.[21] To confirm the sensitivity of the FISH assay, we tested the Namalwa cell line, which contains 2 copies of EBV integrated in each cellular genome.[22] Analysis of 411 cells in 5 separate experiments showed a median of 1 EBV genome per cell and a mean of 0.76 genomes per cell (range, 0-4 copies per cell) (supplemental Figure 1E). This value is slightly lower than the expected number and could be a result of the reduced accessibility of the probe to hybridize to the target when integrated in genomic DNA. Moreover, the 2 copies of EBV are integrated in tandem in the cellular genome of Namalwa cells,[23]

**Table 1. Phenotype of EBV-infected PBMCs from subjects**

| Patient | Diagnosis | EBV DNA load/$10^6$ cells | Percent of EBV-positive cells (no. positive/total no. cells) | | | | |
|---|---|---|---|---|---|---|---|
| | | | B cells | Plasmablast/ plasma cells | Non-B, non-T, nonmonocyte cells | T cells | Monocytes |
| 1 | HIV | 12 000 | 75 (3/4) | ND | 25 (1/4) | 0 | 0 |
| 2 | HIV | 4300 | 89 (8/9) | 0 | 11 (1/9) | 0 | 0 |
| 3 | HIV | 18 000 | 91 (10/11) | 0 | 9 (1/11) | 0 | 0 |
| 4 | HIV | 130,000 | 71 (12/17) | 67 (6/9) | 29 (5/17) | 0 | 0 |
| 5 | HIV | 9400 | 25 (1/4) | 0 | 25 (1/4) | 25 (1/4) | 25 (1/4) |
| 6 | HIV | 5100 | 100 (11/11) | 0 | 0 | 0 | 0 |
| 7 | HIV | 22 000 | 67 (10/15) | 50 (4/8) | 20 (3/15) | 0 | 13 (2/15) |
| 8 | HIV | 6300 | 82 (9/11) | 17 (1/6) | 18 (2/11) | 0 | 0 |
| 9 | Tx | NA | 100 (4/4) | 0 | 0 | 0 | 0 |
| 10 | Tx | 30 000 | 92 (12/13) | 0 | 8 (1/13) | 0 | 0 |
| 11 | Tx | 6200 | 83 (5/6) | ND | 17 (1/6) | 0 | 0 |
| 12 | LyG/HL | 170 000 | 64 (49/77) | 0 | 6 (5/77) | 27 (21/77) | 3 (2/77) |
| 13 | Severe primary EBV infection | 280 000 | 90 (30/33) | 0 | 10 (3/33) | 0 | 0 |
| 14 | PTLD | 1 300 000 | 55 (11/20) | 25 (2/8) | 45 (9/20) | 0 | 0 |
| 15 | ATL EBV-LPD | 190 000 | 79 (19/24) | 21 (3/14) | 21 (5/24) | 0 | 0 |
| 16 | LyG | 28 000 | 79 (15/19) | 14 (1/7) | 21 (4/19) | 0 | 0 |
| 17 | ICL | 110 000 | 97 (28/29) | 0 | 3 (1/29) | 0 | 0 |
| 18 | AA | 64 000 | 80 (8/10) | ND | 20 (2/10) | 0 | 0 |
| 19 | AA | 110 000 | 89 (17/19) | 20 (1/5) | 0 | 0 | 5 (1/19) |
| 20 | AA | 6 500 000 | 52 (24/46) | 37 (6/16) | 48 (22/46) | 0 | 0 |
| 21 | B-cell CAEBV | 15 000 | 73 (11/15) | 20 (1/5) | 27 (4/15) | 0 | 0 |
| 22 | B-cell CAEBV | 30 900 | 97 (29/30) | 0 | 3 (1/30) | 0 | 0 |
| 23 | B-cell CAEBV | 310 000 | 80 (12/15) | 25 (2/8) | 20 (3/15) | 0 | 0 |
| 24 | T-cell CAEBV | 54 666/μg | 0 | ND | 0 | 100 (88/88) | 0 |
| 25 | T-cell CAEBV | 67 612/μg | 0 | ND | 0 | 100 (21/21) | 0 |
| 26 | T-cell CAEBV | 230 000/μg | 0 | ND | 0 | 100 (78/78) | 0 |
| 27 | T-cell CAEBV | 4154/μg | 0 | ND | 0 | 100 (18/18) | 0 |
| 28 | IM | 1700 | 83 (10/12) | 17 (1/6) | 0 | 0 | 0 |
| 29 | IM | 10 651 | 100 (11/11) | 0 | 0 | 0 | 0 |

*For some patients, the percentages for each subpopulation total to > 100%, because the same cell marker (eg, CD20 for B cells) was used in more than one combination* (eg, CD20 with CD3 and CD14 in one combination, CD20 with kappa/lambda in another combination). Patients with HIV infection had CD4 T-cell counts < 400/μL and no EBV-positive lymphomas. Patient 21 received rituximab therapy 1 month before blood was drawn; patients 10, 11, 18, 19, and 20 received anti-thymocyte globulin 5 days to 1 month before blood was drawn (patient 18 received rabbit anti-thymocyte globulin, and patients 10, 11, 18, 19, and 20 received horse anti-thymocyte globulin).

ND indicates not done; Tx, allogeneic hematopoietic stem cell transplant recipient; LyG/HL, lymphomatoid granulomatosis/Hodgkin lymphoma; ATL EBV-LPD, adult T-cell leukemia and EBV-lymphoproliferative disease; ICL, idiopathic CD4 lymphopenia; AA, aplastic anemia receiving antithymocyte globulin; and IM, EBV infectious mononucleosis.

and we may not have been able to resolve the 2 genomes using our Immuno-FISH procedure.

To determine whether the immunofluorescent staining component of Immuno-FISH was sensitive and specific when followed by FISH, we isolated fresh PBMCs and sorted B cells ($CD19^+$), NK cells ($CD56^+/CD3^-$) and T cells ($CD3^+$) by flow cytometry. We stained aliquots of each of the 4 subpopulations with Alexa-conjugated antibodies specific for each subpopulation (eg, T cells with anti-CD3 antibody) and with antibodies that should not recognize the subpopulation (eg, T cells with anti-CD19/anti-CD20). The purity of the staining was more than 97% in all of the combinations tested (supplemental Table 1).

### EBV is detected in circulating B cells

Immuno-FISH was used to characterize the phenotype of the cells infected by EBV from 29 patients with elevated EBV DNA levels in the blood (Table 1). We defined B cells as cells recognized by a combination of anti-CD19 and anti-CD20 antibodies. EBV was detected in B lymphocytes from all 29 patients tested (Figure 1; Table 1), except for the 4 patients with T-cell chronic active EBV (CAEBV) from Japan. In the other 25 patients, B cells represented the majority of cells containing EBV, except for one patient (patient 5) with HIV infection. The median number of EBV genomes in B cells for all the other patients was 13.9 per cell, with a mean of 14.2 per cell (range, 1-40) (Table 2; Figure 2).

### EBV is detected in circulating plasmablasts/plasma cells

Although EBV has been detected in latently infected plasmablastic lymphomas[24] and plasmacytomas in immunocompromised patients with HIV,[25] EBV has not been reported in circulating plasmablasts or plasma cells. Plasmablasts and plasma cells have a prominent cytoplasm containing abundant κ or λ light-chain Ig and lack CD20 on their surface. To determine whether EBV is present in circulating plasmablasts/plasma cells, Immuno-FISH was performed using PBMCs stained with a combination of antibodies to κ and λ chains of Ig and CD20. Surprisingly, we detected EBV in plasmablast/plasma cells in 50% (11 of 22) of the patients tested (Figure 3A; Table 1). Nearly all of the patient groups had some patients with EBV-positive plasmablast/plasma cells. The median number of EBV genomes in plasmablast/plasma cells was 8.3 copies per cell, with a mean of 9.2 copies per cell (range, 3-21), which was lower than the median (13.9) or mean (14.2) number of EBV genomes in B cells (Table 2; Figure 2).

### EBV is detected in circulating T cells in some patients, and in $CD3^+$, $CD4^-$, and $CD8^-$ T cells in Japanese patients with T-cell CAEBV

EBV has been reported in circulating T cells from patients with HIV infection in 1 study based on EBV PCR of sorted T cells[26] and in patients with T-cell CAEBV.[12] Excluding the patients with T-cell

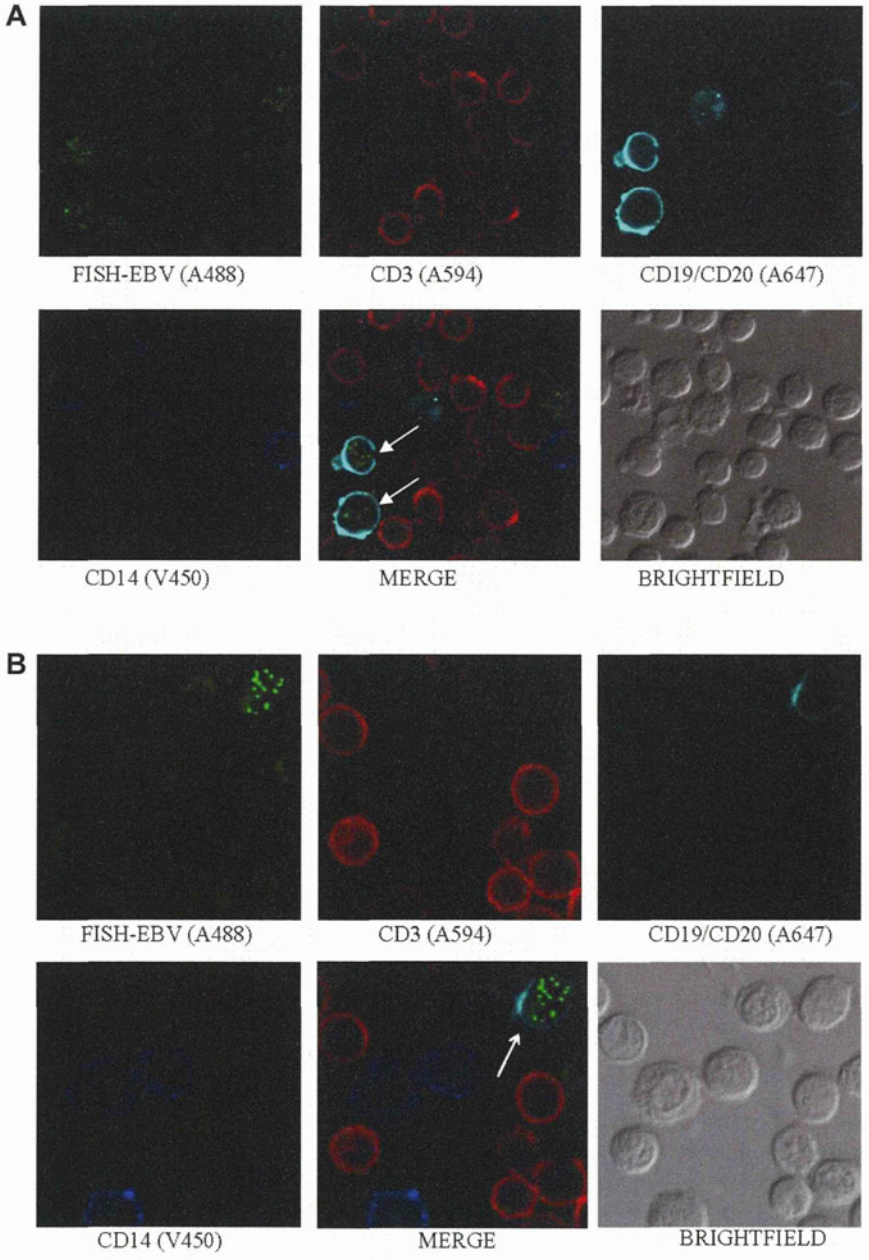


**Figure 1. EBV is detected in B cells.** Photomicrographs of PBMCs stained by Immuno-FISH from patients 17 (A) and 8 (B) show EBV in the nucleus of B cells (arrows). EBV DNA was identified with the biotinylated FISH probe and streptavidin-conjugated Alexa 488, B cells using a combination of Alexa 647–conjugated anti-CD19 and anti-CD20 antibodies (Biolegend), T cells with Alexa 594–conjugated anti-CD3 antibody (Invitrogen), and monocytes with V450-conjugated anti-CD14 antibody (BD Biosciences). Arrows indicate EBV-positive cells.

CAEBV, we detected EBV in T ($CD3^+$) cells from 2 patients: 1 with HIV (patient 5) and 1 with Hodgkin lymphoma (patient 12) (Figure 3B; Table 1). Interestingly, in these patients, the EBV-positive T cells represented more than 25% of their EBV-positive cells. These cells contained a median of 7.85 genomes per cell, with a mean of 9 genomes per cell (range, 2-40). Sufficient cells were available from the patient with Hodgkin lymphoma to perform additional staining of CD4 and CD8 T cells; EBV was only detected in $CD4^+$ T cells, each of which had more than 30 EBV genomes per cell (data not shown). EBV was not detected in T cells from the 7 other patients with HIV.

The EBV receptor in B cells is CD21,[27] whereas in T cells, the virus receptor has not been identified. Although EBV was detected in $CD21^+$ B cells from patient 12 (Figure 4A), none of the EBV-positive, $CD3^+$ cells were also positive for CD21 (Figure 4B).

We also studied 4 patients with T-cell CAEBV from Japan (patients 24-27). Three of 4 patients showed EBV only in $CD3^+$, $CD4^-$, and $CD8^-$ cells (supplemental Figure 2A-B; Table 1). Although the staining for CD4 and CD8 is performed separately from staining for CD3, we can assume that the $CD4^-$, $CD8^-$, and EBV-positive cells (supplemental Figure 2B) are $CD3^+$, because no EBV-positive B cells were detected in these patients. One patient had EBV in $CD3^+$, $CD8^+$, and $CD4^-$ cells (supplemental Figure 2C). The median number of EBV genomes in T cells for the T-cell CAEBV patients was 8.5 copies per cell, with a mean of 9.1 copies per cell (range, 1-26). Combining the results from all 6 patients in whom we detected EBV in T cells,

**Table 2. Mean number of EBV genomes per cell for each cell subpopulation**

| Patient | Diagnosis | EBV DNA load/ $10^6$ cells | Average number of EBV genomes per cell (range) | | | | |
|---|---|---|---|---|---|---|---|
| | | | B cells | Plasmablast/ plasma cells | Non-B, non-T, non-monocyte cells | T cells | Monocytes |
| 1 | HIV | 12 000 | 22.25 (5-40) | ND | 21 (21) | 0 | 0 |
| 2 | HIV | 4300 | 14.75 (6-23) | 0 | 19 (19) | 0 | 0 |
| 3 | HIV | 18 000 | 12.3 (4-24) | 0 | 21 (21) | 0 | 0 |
| 4 | HIV | 130 000 | 15.75 (1-38) | 9.3 (6-16) | 10.4 (6-15) | 0 | 0 |
| 5 | HIV | 9400 | 10 (10) | 0 | 2 (2) | 14 (14) | 2 (2) |
| 6 | HIV | 5100 | 10.9 (4-20) | 0 | 0 | 0 | 0 |
| 7 | HIV | 22 000 | 10.4 (6-17) | 8.7 (4-16) | 8.75 (6-14) | 0 | 1 (1) |
| 8 | HIV | 6300 | 22.4 (5-35) | 16 (16) | 7 (7) | 0 | 0 |
| 9 | Tx | NA | 7.3 (4-11) | 0 | 0 | 0 | 0 |
| 10 | Tx | 30 000 | 14.25 (6-30) | 0 | 28 (28) | 0 | 0 |
| 11 | Tx | 6200 | 16.2 (2-27) | ND | 3 (3) | 0 | 0 |
| 12 | LyG/HL | 170 000 | 17.8 (4-38) | 0 | 11.2 (7-21) | 8.8 (2-40) | 1.5 (1-2) |
| 13 | Severe primary EBV infection | 280 000 | 17.3 (5-35) | 0 | 9.6 (9-10) | 0 | 0 |
| 14 | PTLD | 1 300 000 | 19.2 (3-35) | 7.5 (3-12) | 13 (7-27) | 0 | 0 |
| 15 | ATL EBV-LPD | 190 000 | 10.7 (2-23) | 8.3 (7-10) | 12.5 (10-15) | 0 | 0 |
| 16 | LyG | 28 000 | 8.26 (2-16) | 3 (3) | 18 (8-34) | 0 | 0 |
| 17 | ICL | 110 000 | 12.9 (3-28) | 0 | 25 (25) | 0 | 0 |
| 18 | AA | 64 000 | 16.5 (7-26) | ND | 7 (7) | 0 | 0 |
| 19 | AA | 110 000 | 14.58 (2-34) | 21 (21) | 0 | 0 | 3 (3) |
| 20 | AA | 6 500 000 | 17.04 (3-35) | 10.8 (4-17) | 12.75 (5-21) | 0 | 0 |
| 21 | B-cell CAEBV | 15 000 | 11.18 (4-22) | 6 (6) | 6.3 (2-9) | 0 | 0 |
| 22 | B-cell CAEBV | 30 900 | 13.17 (4-33) | 0 | 5 (5) | 0 | 0 |
| 23 | B-cell CAEBV | 310 000 | 13.9 (6-23) | 5.5 (5-6) | 6 (6) | 0 | 0 |
| 24 | T-cell CAEBV | 54 666/μg | 0 | ND | 0 | 7.25 (1-22) | 0 |
| 25 | T-cell CAEBV | 67 612/μg | 0 | ND | 0 | 7.66 (1-17) | 0 |
| 26 | T-cell CAEBV | 230 000/μg | 0 | ND | 0 | 10.24 (2-26) | 0 |
| 27 | T-cell CAEBV | 4154/μg | 0 | ND | 0 | 9.88 (3-21) | 0 |
| 28 | IM | 1700 | 12.5 (9-22) | 5 (4-6) | 0 | 0 | 0 |
| 29 | IM | 10 651 | 12.63 (5-27) | 0 | 0 | 0 | 0 |

the mean copy number of EBV genomes in T cells was lower than the mean copy number for B cells; however, the difference was not significant (paired *t* test, $P = .77$; Figure 2).

### EBV is detected in circulating monocytes

EBV has been reported to infect circulating monocytes of patients with HIV.[15] We detected EBV in monocytes ($CD14^+$ cells) from 4 patients: 2 HIV-positive patients, 1 with Hodgkin lymphoma, and 1 receiving antithymocyte globulin for aplastic anemia (Figure 5A; Table 1). The median number of EBV genomes in monocytes for the 4 patients was 1.75 copies per cell, with a mean of 1.85 copies per cell (range, 1-3). This was significantly lower than the mean copy number for B cells (paired *t* test; $P = .0083$) (Figure 2).

### EBV is not detected in circulating NK cells in the patients in this study

EBV has been detected in circulating NK cells of patients with NK-cell CAEBV.[12] When PBMCs from the patients were stained with a combination of antibodies to CD16 and CD56, NK cells ($CD16^+/CD56^+$ and $CD3^-$) were detected in each of the patients; however, none contained EBV.

### EBV is detected in circulating "non-B, non-T, and non-monocyte cells"

Surprisingly, in 69% of the patients, we detected EBV in PBMCs that were not recognized by B-cell (CD19, CD20), T-cell (CD3), or monocyte (CD14) monoclonal antibodies (Figure 5B; Table 1). Several patients, including some with HIV (patients 1, 4, 5, and 7), PTLD (patient 14), aplastic anemia receiving antithymocyte globulin (patients 18 and 20), and B-cell CAEBV (patients 21 and 23) had EBV in non-B, non-T, and non-monocyte cells that represented more than 20% of EBV-positive cells. EBV was detected in this cell population in each of the groups of patients we studied, except for patients with T-cell CAEBV from Japan and patients with infectious mononucleosis (IM). The median number of EBV genomes in non-B, non-T, non-monocyte cells for all the patients was 10.8 copies per cell, with a mean of 12.3 copies per cell (range, 2-34). Comparison of the mean copy number in EBV-positive B cells versus EBV-positive non-B, non-T, non-monocyte cells showed no significant difference (paired *t* test; $P = .197$; Figure 2).

### EBV lytic protein BZLF1 is detected in circulating PBMCs

To determine whether we could detect evidence for lytic replication of EBV in virus-infected PBMCs, we performed immunofluorescence staining for EBV BZLF1 (an immediate-early protein that mediates the switch between the latent and the lytic forms of EBV infection), together with T- and B-cell markers (CD3 and CD19/CD20). Sufficient cells were available to assay 15 of the 29 patients (patients 8, 11, 12, 14, 15, 19-23, and 25-29). We detected BZLF1 in 87% (13 of 15) of these patients tested, indicating lytic EBV replication. The cell-surface phenotype of the BZLF1-positive cells was variable: in 4 patients, some of the BZLF1-positive cells were $CD19^+/CD20^+$, whereas other cells were negative for both CD19/CD20 and CD3 (patients 8, 14, 15, and 21); in 3 patients, some BZLF1-positive cells were $CD3^+$, whereas others were negative for both CD19/CD20 and CD3 (patients 12, 26, and 27) (Figure 6). In 6 patients (patients 11, 19, 22, 23, 28, and

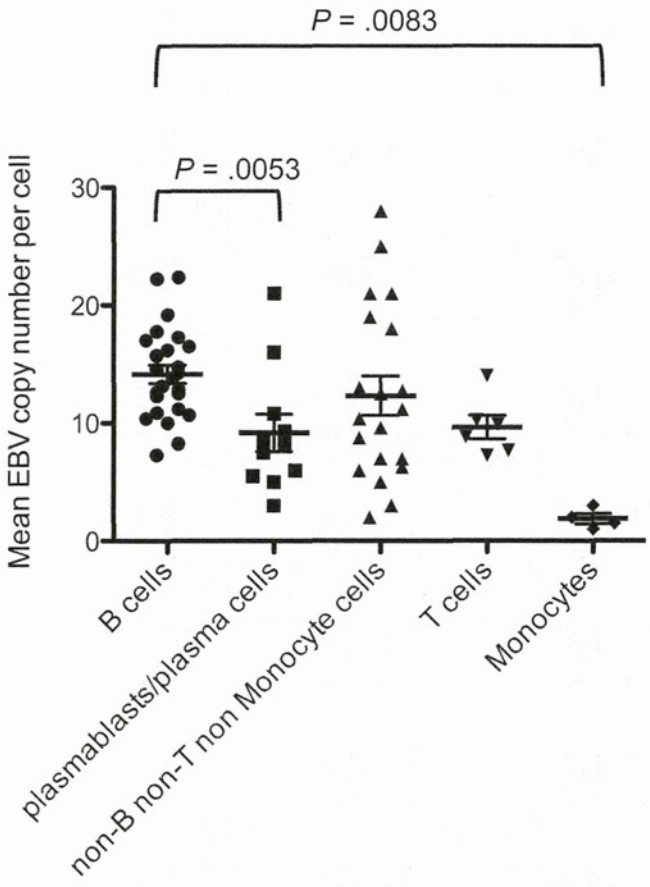


**Figure 2. Mean EBV copy number per cell for each cell subpopulation for each patient.** *P* values were obtained with the *t* test. The difference in mean EBV copy number between B cells and non-B, non-T, non-monocyte cells ($P = .2878$) and between B and T cells ($P = .77$) was not significant.

29), all of the BZLF1-positive cells were negative for CD3 and CD19/CD20.

### Correlation between EBV copy number per cell and underlying disease

We analyzed the distribution of EBV copy numbers per cell for each of the 29 patients (Tables 2-3). Half of the patients infected with HIV had cells carrying more than 30 EBV genomes per cell; however, high copy numbers per cell did not correlate with the EBV DNA load in the blood (supplemental Figure S3). Some patients with high EBV DNA loads (patients 7 and 10 with 22 000 and 30 000 EBV genome copies per million cells, respectively) had no cells with more than 30 EBV genome copies, whereas others with lower EBV DNA loads (patients 6 and 8 with 5100 and 6300 EBV genome copies per million cells, respectively) had cells with more than 30 EBV genome copies (Table 3). Moreover, the percentage of cells with more than 30 EBV genome copies in some patients with a lower EBV DNA load (patient 1 with 20% of cells with more than 30 EBV genomes and 12 000 copies of EBV per million cells) was higher than in patients with a high EBV DNA load (patient 4 with 8% of cells with more than 30 EBV genomes and 130 000 copies of EBV per million cells). Only one patient in our study, HIV patient 1, had a majority of EBV-positive cells with more than 20 EBV genomes per cell.

Only patients with HIV (patients 1, 3, and 8) and those receiving antithymocyte globulin for aplastic anemia (patients 19 and 20) had more than 25% of EBV-positive cells with more than 21 EBV genomes per cell.

Analysis of the 7 patients with B- or T-cell CAEBV showed that only one of these patients (patient 22) had more than 30 EBV genomes per cell. Despite the high EBV loads in these patients, 6 of 7 patients had a majority of EBV-positive cells with only 1-10 EBV genomes per cell. Thus, in these patients, the high EBV DNA load was caused by a large number of EBV-infected cells, rather than a high copy number per cell. Similarly, the 2 patients with IM also had a majority of EBV-positive cells with 10 or fewer EBV genomes per cell.

We also analyzed the distribution of the EBV genome copies per cell based on their phenotype. The mean number of EBV genome copies per cell for each of the different cell types showed no correlation with the total EBV DNA load in the blood (Figure 7). A more detailed analysis of the distribution of the number of EBV copies in B cells also showed no correlation with the EBV DNA load in the blood (Table 3; supplemental Figure S4). Taken together, these results suggest that patients with higher EBV DNA loads have a higher number of virus-infected cells, rather than a higher number of EBV genome copies per cell.

## Discussion

Using the Immuno-FISH procedure, we analyzed 29 patients with different diseases that had high EBV DNA loads in the peripheral blood. All of the patients, except for the 4 T-cell CAEBV patients from Japan, were expected to have a B-cell EBV lymphoproliferative process. In all but 1 of these 25 patients (HIV patient 5), the majority of the EBV-positive cells were B cells; however, there was a wide range (52%-100% of the EBV-positive cells were B cells). Using this technique, EBV was detected in both B and non-B cells in 88% of these patients. Thus, the generally accepted belief that EBV is usually present only in B cells is not the case for patients with elevated EBV DNA loads.

Circulating plasmablast/plasma cells are detected in the blood of healthy persons, although they represent approximately 0.14% of PBMCs.[28] Plasmablast/plasma cells have been detected in the blood in patients with virus infections,[29] and these cells represent 5.5% of B cells in the peripheral blood of patients with HIV viremia.[30] EBV has been detected in plasma cells in human tonsils; approximately 10%-20% of these cells undergo lytic virus replication and most do not complete the full cycle.[31]We detected EBV in plasmablasts/plasma cells in the blood of approximately 50% of the patients. Therefore, in patients with lymphoproliferative diseases and high EBV DNA loads, EBV is present in circulating plasmablasts/plasma cells, in addition to B cells.

We detected EBV in peripheral blood T cells in a patient with HIV and in one with Hodgkin lymphoma, as well as in the 4 Japanese patients with T-cell CAEBV. Using cell sorting followed by PCR, EBV was found in circulating T cells in HIV-1–infected children and adolescents with elevated EBV DNA loads.[26] EBV was found in $CD4^+$ and $CD8^+$ cells at approximately 10-fold lower EBV copy numbers than in $CD19^+$ cells. In addition to T-cell CAEBV,[12,13] EBV has been detected in T cells from patients with EBV-associated hemophagocytic lymphohistiocytosis[32] and from patients with T-cell lymphoma.[33,34] In contrast to the EBV-infected B cells, we were unable to detect CD21 on EBV-infected T cells. CD21 has been detected on the surface of T-cell lines[35] and at low levels on primary T cells.[36] Infection of a human T-lymphoblastic cell line resulted in virus internalization and viral